Accepted Manuscript

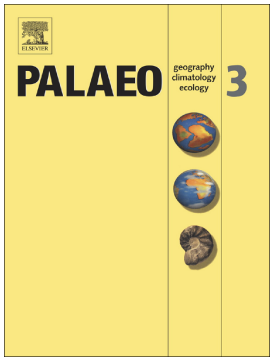

Unravelling hinterland and offshore palaeogeography from pre-to-syn-orogenic clastic sequences of the Betic Cordillera (Sierra Espuña), Spain

Francesco Perri, Salvatore Critelli, Manuel Martín-Martín, Stefano Montone, Ugo Amendola

PII: S0031-0182(16)30800-8
DOI: doi: 10.1016/j.palaeo.2016.11.049
Reference: PALAEO 8084

To appear in: *Palaeogeography, Palaeoclimatology, Palaeoecology*

Received date: 1 July 2016
Revised date: 24 November 2016
Accepted date: 29 November 2016

Please cite this article as: Francesco Perri, Salvatore Critelli, Manuel Martín-Martín, Stefano Montone, Ugo Amendola , Unravelling hinterland and offshore palaeogeography from pre-to-syn-orogenic clastic sequences of the Betic Cordillera (Sierra Espuña), Spain. The address for the corresponding author was captured as affiliation for all authors. Please check if appropriate. Palaeo(2016), doi: 10.1016/j.palaeo.2016.11.049

This is a PDF file of an unedited manuscript that has been accepted for publication. As a service to our customers we are providing this early version of the manuscript. The manuscript will undergo copyediting, typesetting, and review of the resulting proof before it is published in its final form. Please note that during the production process errors may be discovered which could affect the content, and all legal disclaimers that apply to the journal pertain.

ACCEPTED MANUSCRIPT

Unravelling hinterland and offshore palaeogeography from pre-to-syn-orogenic clastic sequences of the Betic Cordillera (Sierra Espuña), Spain

Francesco Perri[a], Salvatore Critelli[a*], Manuel Martín-Martín[b], Stefano Montone[a], Ugo Amendola[a]

[a]*Dipartimento di Biologia, Ecologia e Scienze della Terra, Università della Calabria, 87036 Arcavacata di Rende (CS), Italy*

[b]*Departamento de Ciencias de la Tierra y del Medio Ambiente, Universidad de Alicante, Ap. 99, E-03080 Alicante, Spain*

*Corresponding author:
E-mail address: salvatore.critelli@unical.it (S. Critelli)
Tel.: +39 0984 493678

ACCEPTED MANUSCRIPT

Abstract

The Malaguide Complex (Betic Cordillera) occurs in the Sierra Espuña area (SE Spain) providing a favorable setting to study a sedimentary successions from continental and shallow-marine to deep-marine environments using structural and stratigraphic relations, and petrological and geochemical signatures. The aim of this work is to outline the sedimentary evolution of the Malaguide Complex and the El Niño Fm. This succession is arranged into pre-orogenic (Palocene-Early Oligocene) and syn-orogenic (Late Oligocene-Early Miocene) stages. The detrital modes of sandstones of the overall succession are heterogeneous and indicate a multi-source area, marked by exhumation till an unknown Malaguide basement and probably lower units of the Internal Betic Zone (e.g. Alpujarride Complex) in the case of the El Niño Fm. Pre-orogenic deposits are mainly carbonate with abundant skeletons of intrabasinal to extra-basinal larger foraminifera, calcareous lithic fragments and quartz grains, and metamorphic lithic fragments. Minor metamorphic lithic fragments occur in the Eocene deposits (i.e. Espuña Fm). Calcareous lithic fragments and extra-basinal fossils (lithoclastic bioclasts) are mostly present in the Early Oligocene pre-orogenic formations (i.e. As Fm) and were derived from the Paleocene-Eocene sedimentary successions of the Malaguide Complex. Syn-orogenic sandstones are quartzolithic with abundant metamorphic and sedimentary lithic fragments

ACCEPTED MANUSCRIPT

(slate, phyllite, fine-grained schist, ooidal grainstone, mudrock and quartz-rich siltstone fragments). Sedimentary lithic fragments were derived from the Mesozoic successions of the Malaguide Complex while metamorphic detritus is related to the Malaguide basement (probably also Alpujarride from Burdigalian on) that was exhumed starting from the Late Oligocene. Mudrocks of the syn-orogenic clastics, record an increase of phyllosilicate, quartz and feldspars and an abrupt decrease in calcite and dolomite. The abundance of calcite and dolomite, and traces of hematite occur dominantly in the pre-orogenic mudrocks. The geochemical signatures suggest a provenance mostly derived from felsic source rocks with a minor supply from mafic metavolcanic rocks in some samples of the syn-orogenic stage. The syn-orogenic formations (i.e. Rio Pliego Fm and El Niño Fm) are characterized by higher Cr/V values than the pre-orogenic formations suggesting a mafic supply for the syn-orogenic samples. In particular, the contents of Cr (average=85 ppm) and Ni (average=48 ppm) for the samples of the Rio Pliego and El Niño Formations are higher than those samples (Cr average=20 ppm; Ni average=14 ppm) of the pre-orogenic formations. Palaeoweathering indices suggest low to moderate weathering conditions for the source area(s). The Cenozoic studied succession played a key role in the geodynamic evolution of the Betic Cordillera, representing the key tectonic element of the western Mesomediterranean domains.

Keywords: Cenozoic Malaguide Complex; Betic Cordillera; sandstone detrital modes; mudrock; provenance; geodynamic evolution

ACCEPTED MANUSCRIPT

ACCEPTED MANUSCRIPT

1. Introduction

The Sierra Espuña area is located to the west of the Murcia province in SE Spain (Fig. 1C), belonging to the Internal Betic Zone (IBZ). The IBZ is mainly made of a tectonic nappe stack formed, from bottom to top, by the Nevado-Filabride, Alpujarride and Malaguide Complexes (Fig. 1B). Both, the Nevado-Filabride and the Alpujarride Complexes are affected by Alpine (and pre-Alpine) metamorphism, whereas the Malaguide is slightly (the older basement) or not at all affected (Martín-Algarra, 1987; Sánchez-Navas et al., 2012, 2014,).

The tectonic stacking and the alpine metamorphism of the IBZ is the response to a continental collision (Guerrera and Martín-Martín, 2014) of the Mesomediterranean Microplate (MM: responsible of the Alpujarride and Malaguide Complexes) against the South Iberian Margin (External Betic Zone - EBZ - subdivided in the Subbetic and Prebetic units) involving the Nevado-Filabride oceanic branch (subducted bellow the MM) (*e.g.*, Perrone et al., 2006; Critelli et al., 2008; Perri, 2014; Perri et al., 2013, 2016b) (Fig. 1D). The Malaguide Complex was related to the Kabylian and Calabrian Internal units, and all of them constituted the southern part of the MM (Martín-Martín et al., 2006a) to the N of the Maghrebian Flysch Basin (*e.g.*, Boullin 1986; Guerrera et al., 2005; El Talibi et al., 2014 and references therein). This basin separated the MM from Africa during the Mesozoic and part of the Cenozoic (Fig. 1D).

The Internal Betic Zones together with the alpine chains (Fig. 1A) of the Circum-Mediterranean belts (i.e. Rif, Tell, Calabria-Peloritani and Apennine chains) were formed after the breakoff of the previously deformed MM (which had formed a laterally continuous orogenic belt called AlKaPeCa: Bouillin et al., 1986; Guerrera et al., 1993), which opened the Western Mediterranean basins during the Miocene (Critelli et al., 2008; Guerrera et al., 2012; Alcalá et al., 2013; Guerrera and Martín-Martín, 2014; Guerrera et al., 2015). Moreover, these Internal Zones had a quite similar Meso-Cenozoic geologic evolution. These facts and the occurrence of a thick, continuous, unmetamorphosed and complete sedimentary Meso-Cenozoic cover over the Malaguide Complex makes the Sierra Espuña area very important for correlations among of them, allowing the increase of knowledge on the Paleogene to Early Miocene paleogeographic and geodynamic evolution of the central-western Mediterranean region. The aim of this paper is to discuss the stratigraphic relations and the compositional signatures of Paleocene to Burdigalian arenites and mudrocks of the stratigraphic cover of the Malaguide Complex that constrain the tectonic history of the Betic Cordillera orogenic accretionary processes and related foreland basin system.

2. Geological settings

ACCEPTED MANUSCRIPT

The study area includes the Sierra Espuña mountain area and the Mula-Pliego Basin located to the NE of it (Figs. 2 and 3A). The Sierra Espuña mountain area constitutes an antiformal stack of Malaguide and Alpujarride tectonic units, followed, towards the N, by a great sinclinorium in the basin, including several smaller folding and thrusting structures forming structural culminations exclusively made of Malaguide Paleogene to Lower Miocene Rocks (Martín-Martín and Martín-Algarra, 2002; Martín-Martín et al., 2006a; Martín-Rojas et al., 2007). The detachment level of the thrusts of the entire area is the Paleozoic-Triassic boundary (Martín-Martín and Martín-Algarra, 2002).

The antiformal stack is constituted, from bottom to top, by one Alpujarride tectonic unit, two intermediate Alpujarride-Malaguide units and three Malaguide units. The two Malaguide upper units (Morrón de Totana and Perona) include a Triassic to Tertiary sedimentary cover.

The Morrón de Totana unit bears at its base a thin Carboniferous basement of slates and graywackes in tectonic contact onto the Mesozoic succession of the La Santa Malaguide tectonic unit, and this is followed by the thickest and most continuous Meso-Cenozoic succession of the Malaguide Complex (Martín-Martín et al., 2006a). The Mesozoic succession is more than 2000 meters thick and is made up of Triassic and Jurassic sediments followed by a thin Cretaceous succession (Martín-Martín et al., 2006a; Caracuel et al., 2006). The Triassic succession (Martín-Martín et al., 2006a; Perrone et al., 2006; Critelli et al., 2008; Perri 2014; Perri and Ohta, 2014; Perri et al., 2013), unconformable onto the Paleozoic, is made of continental redbeds with carbonatic and conglomeratic intercalations arranged into three main depositional sequences. The Triassic succession has been interpreted as belonging to shallow marine-transitional and continental realms. The Triassic succession gradually changes upwards to the Jurassic succession due to a marine transgression and is made of dolostones, at the base, followed by several limestone facies evolving upward into nodular limestones in the Late Jurassic (Cecca et al., 2002; Caracuel et al., 2006; Martín-Martín et al., 2006b; Critelli et al., 2008). The entire succession is interpreted as the evolution of a marine platform to a slope realm in the upper part. The thin Cretaceous succession (Caracuel et al., 2006) shows Berriasian limestones appearing in continuity over the Late Jurassic succession. After a stratigraphic gap, these are followed by a sandy glauconite-rich level Albian in age followed by Upper Cretaceous marly-limestones and marls (Paquet, 1969). The Mesozoic succession is topped by an unconformity followed by a thick (more than 1000 m) Paleocene to Early Miocene succession (aim of this research), one of the most developed and best preserved of the Internal Zones of the central-western mediterranean area.

ACCEPTED MANUSCRIPT

3. Stratigraphic insights of the Paleocene to Lower Miocene succession

The Paleocene to Lower Miocene succession of the Sierra Espuña area is made up of several formations evolving from continental and shallow marine, to deep marine realms (Martín-Martín et al., 1997a, b, c; Martín-Martín et al., 1998; Serra-Kiel et al., 1998). According to the former authors the succession is divided into two sedimentary cycles (pre-orogenic and syn-orogenic, respectively) and, in turn, arranged into several depositional sequences with stratigraphic formations, as it follows (Figs. 3A and 4).

3.1 Pre-orogenic cycle (Paleocene to Early Oligocene)

The pre-orogenic cycle includes Paleocene, Cuisian-Early Lutetian, Middle Lutetian-Priabonian and Early Oligocene depositional sequences.

Paleocene Depositional Sequence. This sequence consists of the Mula Fm, which is composed of unconformable continental redbeds with calcareous clays and conglomerates rich in *microcodium* (Garumnian-like facies: Arribas et al., 1996) in the Sierra Espuña area and, in the Mula-Pliego Basin, of shallow marine grayish silts with dark limestones and calcarenites rich in larger foraminifera and little bivalves, evolving upward to dark-blue marls with planktonic foraminifera (Fig. 3B).

Cuisian to Early Lutetian Depositional Sequence. It overlies, unconformably and transgressively, the previous sequence and is composed of two sedimentary formations related by a lateral change of facies: 1) The Espuña Fm is made of cream coloured and white limestones and sandy limestones with alveolines and nummulitids (Fig. 3C); 2) The Valdelaparra Fm (only outcrops in the Sierra Espuña s.s. area) is made of continental to marshy grey-blue marls and marly limestones with gastropods and bivalves, and containing lignite-bearing levels.

Middle Lutetian to Priabonian Depositional Sequence. It lies also unconformable and transgressive onto the previous depositional sequence and consists of two sedimentary formations, related by lateral and upward change of facies. The Malvariche Fm (Middle Lutetian to Early Bartonian) constitutes its lower part and consists of brownish to reddish calcarenites with sandy-marly intercalations, both with numerous oversized larger foraminifera (Fig. 3D). It changes, both laterally and upward, to the Canovas Fm (Late Bartonian to Priabonian) and it consists of open-marine pinkish to yellowish marls and silts with foraminifera.

Early Oligocene Depositional Sequence. It is represented by the As Formation, which is composed of limestone conglomerates (Fig. 3E) and shallow-water calcarenites and marls, both containing

ACCEPTED MANUSCRIPT

abundant rounded quartz pebbles and numerous reworked larger foraminifera. This depositional sequence is transgressive, and it overlies the former depositional sequences. It is the youngest formation of the pre-orogenic cycle since it is involved in the main thrusts of the tectonic stacking of the area.

3.2 Syn-orogenic cycle (Late Oligocene to Early Miocene)

The syn-orogenic cycle is made up by the Late Oligocene-Aquitanian and the Burdigalian *p.p.* depositional sequences.

Late Oligocene to Aquitanian Depositional Sequence. This sequence can be considered the upper one properly related to the Malaguide Complex. Two transgressive and unconformable formations overlie the former succession, and they appear related by a lateral but upwardly change of facies. In the lower part and mainly outcropping in the Sierra Espuña area the Bosque Fm and is made of limestone conglomerates, algal limestones, and yellowish to whitish bioclastic calcarenites (Fig. 3F). The Bosque Fm evolves upward into silty marls with local calcarenite intercalations. This formation was deposited in transitional (fan delta) to shallow marine (platform) environments that, both laterally and vertically, change gradually to the deep-marine beds of the Rio Pliego Fm (only in the Mula-Pliego Basin) consisting of reddish to pinkish micaceous marls, clays, silts, turbiditic sandstones, and polygenic olistostromes including pebble- to cobble-, locally boulder- sized clasts of Paleozoic and Triassic rock eroded from the Malaguide substratum (Fig. 3G).

Burdigalian p.p. Depositional Sequence. This sequence, as part of the Viñuela Group (Matín-Algarra, 1987), is considered in the whole IBZ as a transgressive one deposited after the structuring of the IBZ, and later to the metamorphism in the lower units. It appears only in the Mula-Pliego Basin with a sharp contact above the Rio Pliego Fm. It includes greenish to grayish micaceous marls, sandstones, and siliceous pelites with silexite levels (Fig. 3H), Early to Middle Burdigalian in age, and defined as the El Niño Fm. This depositional sequence in the area is overthrust by the EBZ in the Internal-External zone boundary of the eastern Betic Zone. This main contact is overlain by the Late Burdigalian to Serravallian late-orogenic succession sealing the tectonic contact (Tent-Manclús et al., 2001).

4. Analytical methods

ACCEPTED MANUSCRIPT

Sandstone and mudrock samples of the Paleocene to Burdigalian succession of the Sierra Espuña area were collected to cover the entire sedimentary succession (Figs. 2, 3, 4 and 5). The sampling was concentrated in those parts of the succession that are better exposed and preserved and thicker than in other analogue areas of the Malaguide Complex. For the purpose of this study, siliciclastic and carbonatoclastic samples have been selected. In particular, the prevalence of carbonate components is specifically related to many formations of the succession and is strongly evident in the field, from the presence of carbonate clasts and bioclasts.

For coarse-medium grained siliciclastic sandstones, more than 300 points were point-counted, according to the Gazzi-Dickinson method (Gazzi, 1966; Dickinson, 1970; Ingersoll et al., 1984; Zuffa, 1985). Sandstone detrital modes are defined according to Dickinson (1970), Ingersoll and Suczek (1979), Zuffa (1985), Critelli and Le Pera (1994), Critelli and Ingersoll (1995) and Critelli et al. (2007). Carbonate samples have been described according to the Dunham (1962) classification, as revised by Embry and Klovan (1971). Some calcarenite and calcirudite samples were counted through a semi-quantitative method, using Baccelle and Bosellini (1965) charts.

Mudrock samples were crushed and milled in an agate mill to a very fine powder. Furthermore, the powder was placed in an ultrasonic bath at low power for a few minutes for disaggregation.

The mineralogy of the whole-rock powder was determined by X-ray diffraction (XRD) using a Bruker D8 Advance diffractometer (CuKα radiation, graphite secondary monochromator, sample spinner; step size 0.02; speed 1 sec for step) at the Università della Calabria (Italy). Semiquantitative mineralogical analysis of the bulk rock was carried out on random powders measuring peak areas using the WINFIT computer program (Krumm, 1996). The weight percentage of each mineral was obtained according to the procedure proposed by Cavalcante et al. (2007). The chemical composition of the studied mudrocks was determined by X-ray fluorescence spectrometry (XRF) using a Bruker S8 Tiger equipment at the Università della Calabria. Total loss on ignition (L.O.I.) was obtained after heating the samples for 3 h at 900 °C.

5. Petrological and detrital modes of sandstones and rudstones

Raw point-count data of sandstones in Table 1, and the recalculated modal point-count data are in Table 2.

5.1 Pre-orogenic arenites

ACCEPTED MANUSCRIPT

Medium to fine-grained arenites of the pre-orogenic sedimentary sequence are carbonatoclastic bearing although an important siliciclastic component also occurs (Figs. 6 and 7).

The Paleocene Depositional Sequence (Mula Fm) contains bioclastic limestones with grainstone and packstone and locally rudstone textures are dominant. *Rodoficean* algae, *Bryozoan*, bivalve and crinoid fragments, and foraminifers typical of external margin of a shallow-marine platform, represent the main skeletal constituents. *Rodoficean* fragments mainly appear as gravel to coarse sand-size subrounded and spherical grains, whereas *Bryozoans* and other bioclasts are more angular and locally recrystallized by sparitic cement. Extrabasinal carbonate fragments (CE; *sensu* Zuffa, 1980) are present as subrounded to angular grains, partially bordered by algal crusts. They are composed of bioclastic wacke/mudrocks including benthic foraminifers, *Rodoficean* algae and locally Microcodium-type grains. Siliciclastic particles are present in fine-grained sandstones and siltstones (3P sample). They contain fine sand to silt-size quartz grains, mainly as subrounded to angular and subspherical monocrystalline grains, rare polycrystalline quartz with tectonic-fabric, micas (biotite and muscovite), and bioclasts (planktonic and benthic foraminifers, echinodermata and bivalve fragments). Such siliciclastic samples are well sorted, have poor porosity and some detrital grains generally have more contacts with neighboring grains, indicating an initial mechanical compaction. The matrix is represented by brown siltstone and dark-yellow altered clayey inclusions, indicating partial subaerial exposure, and is locally recrystallized by silt-sized calcite spars. *Microcodium*-type recrystallization features have been observed.

The Cuisian to Early Lutetian Depositional Sequence (Espuña and Valdelaparra Fms) includes basal mixed carbonate and siliciclastic arenites (hybrid arenites *sensu* Zuffa, 1980; Critelli et al., 2007) followed by bioclastic limestones with packstone textures. The intrabasinal carbonate component (CI) is more abundant (Espuña Fm: $NCE_{38}CI_{62}CE_0$; Zuffa, 1980; Fig. 6) and largely increases toward the top where bioclastic limestones occur. *Alveolinas*, *Nummulites* and, less frequently, *Assilinas*, Echinodermata fragments and gastropods shells are the main biotic assemblage of the studied Espuña Fm. The siliciclastic grains are present in the lower layers of Espuña Fm and are quartzarenites ($Qm_{96}F_0Lt+CE_4$; Dickinson, 1970; Fig. 6). Quartz grains mainly appear as medium sand-size, and they are monocrystalline subrounded to subspherical grains with locally internal abrasions and muscovite inclusions. They are well sorted and generally have tangential contacts with neighboring grains. Polycrystalline grains are minor and have similar tectonic-fabric. Few traces of phaneritic plutonic and medium to high-grade metamorphic rock fragments are also present. The interstitial component of Espuña Fm hybrid arenites mainly include calcite cement, represented by either clast-rim fringe and pore-filling blocky sparitic types, and rare authigenic minerals like pore-lining clays, as well as quartz overgrowths. Synthaxial cements growing around

ACCEPTED MANUSCRIPT

Echinodermata fragments are also present. The matrix of bioclastical limestones include dark-brown micrite, locally recrystallized, probably during phases of deep burial diagenesis.

The Middle Lutetian to Priabonian Depositional Sequence (Malvariche and Cánovas Fms) is mainly made of calcirudite/calcarenite strata and siltstones. Calcirudites are mainly composed of gravel to coarse-sand size skeletons of *Nummulites* and *Discocyclinas*, and secondary crinoid and bivalve fragments. *Rodoficean* bioclasts fragments and Miliolinid foraminifers also occur. *Nummulites*, up to 10 cm of diameter, reach 60-70% of abundance and appear as well preserved grains with inner chambers filled dominantly by sparitic cements and secondary by micrite and glauconitic cement. *Discocyclina* bioclasts and fossils are locally angular, and their amount slightly increases toward the top of the Malvariche Formation (from 10 to 30%; sample 11P). *Alveolina* bioclasts are totally missing. The interstitial component includes both carbonate matrix and cement. The matrix is composed of fine to sand size calcite grains, probably derived from disarticulation of benthic macro foraminifers, and also silt-size quartz and mica grains, floating into dark-brown micrite that is partially recrystallized to a pseudosparitic cement. Several joints, filled by sparitic cement and recent brown clayey inclusions are evident. The carbonate cement consists of blocky calcite spars filling pores and fibrous fringe cements on skeletal grains. Siltstones are made of quartz grains and minor micas grains with benthic foraminifa. Their interstitial component is composed by microsparitic calcite cement.

The Early Oligocene Depositional Sequence (As Fm) shows that the siliciclastic content slightly increases (As Fm: $NCE_{51}CI_2CE_{47}$; Zuffa, 1980), as well as extrabasinal carbonate grains, although the composition always remains quartzarenitic (As Fm: $Qm_{92}F_0Lt+CE_8$ Dickinson, 1970; Fig. 6). Such arenites include monocrystalline quartz grains, rare tectonic-fabric polycrystalline quartz, phaneritic metamorphic rock fragments and chert. The carbonate component is mainly of extrabasinal origin (CE) and is composed by Paleocene-Eocene bioclasts of *Nummilites*, *Discocyclinas, Bryozoan* and *Rodoficean* algae, and subrounded to angular carbonate lithic fragments (CE). These latter constituents consist of bioclastic wacke/mudrocks with *Bryozoans*, *Rodoficean* algae and minor bivalves, *Alveolinas* and Miliolinid foraminifers. Echinodermata fragments, included as intrabasinal carbonate component (CI), also occur. These sandstones are poorly-to-moderate sorted. Several grains have tangential and minor sutural contacts. The interstitial component is totally filled by sparitic calcite cement that locally replaces some grains (poikilotopic calcite). A few joints filled by sparitic calcite cement are also present.

5.2 Syn-orogenic arenites

ACCEPTED MANUSCRIPT

Sandstone detrital modes for the syn-orogenic cycle abruptly changed from carbonate-rich to siliciclastic rocks.

The Late Oligocene to Aquitanian Depositional Sequence (Bosque and Rio Pliego Fms) contains only bioclastic calcarenites in the Bosque Fm. They mainly comprise reworked Paleocene-Eocene bioclasts (CE), including single angular and broken skeletons of *Nummulites* and *Discocyclinas*, up to 40-50% in abundance along with 20% extrabasinal lithic fragments (CE). These latter grains are characterized by rounded and subspherical to flattened grains of bioclastic wackestones and mudstones, including sponge spicules, radiolarians and foraminifers. Angular polygonal-shape fragments of shallow-marine carbonates with grainstone texture, comprising internal micritized ooids, secondary oncoids and bivalves in addition occur. Also, Lepidocyclinids and *Nephrolepidina praemarginata* skeletons, which have Chattian-Aquitanian age, and Echinodermata fragments also occur. The siliciclastic component is minor and only represented by fine-sand size monocrystalline quartz grains. These calcarenites are poorly sorted and several grains have tangential and minor sutural contacts with neighboring grains, indicating a strong mechanical compaction. The interstitial component includes sparitic calcite cement, which locally replaces some bioclasts and carbonate lithic fragments.

The onset of increasing siliciclastic content occurs in the upper part of the Bosque Fm, where siltstones, rich in quartz and micas, are present. The lateral and overlying Rio Pliego Fm is mainly siliciclastic. It is composed of fine-grained sandstones *(*lower part), followed by coarse-grained sandstones and micro-conglomerates (middle part). They are capped by fine-grained sandstones and siltstones (upper part).

In the lower Rio Pliego Fm, sandstones are quartzolithic ($Qm_{56}F_0Lt+CE_{44}$; Fig. 6). They mainly include monocrystalline quartz grains, appearing mainly as spherical and angular monocrystalline grains and polycrystalline grains with a prevalence of tectonic-fabric grains (2 to 8%). Metamorphic lithic fragments are abundant and include phyllite, slate and fine-grained schist (aphanitic) and rare metarenites (phaneritic). Sedimentary lithic fragments (Lss) are minor as such as chert. Extrabasinal carbonate grains (CE), up to 10%, mainly consist of angular *Nummulite* skeletons, *Rodoficean* algae, benthonic foraminifers (Nodosaridae) and carbonate lithic fragments of bioclastic wackestone/mudstone including thin-shelled bivalves and ostracods. The matrix is chiefly siliciclastic and is composed of silt-sized angular quartz grains floating in a dark-brown reddish siltstone with clayey inclusions.

Samples from coarse-grained sandstones and micro-conglomerates (from 17 to 21P) have a homogeneous quartzolithic ($Qm_{26}F_0Lt+CE_{74}$; Fig. 6) composition and therefore they can be

ACCEPTED MANUSCRIPT

included in a specific sandstone petrofacies, named Rio Pliego petrofacies. These sandstones have variable non-carbonate versus carbonate extrabasinal lithic fragments with a general dominance of siliciclastic content ($NCE_{73}CI_1CE_{26}$; Tab. 2). Similarly, they have variable sedimentary and carbonate versus metamorphic lithic fragments (average value; $Lm_{41}Lss_{29}Lsc_{30}$,; $Rg_0Rs_{55}Rm_{45}$, Fig. 6) with a slight dominance of metamorphic grains. Quartz grains are not abundant and are mainly present as monocrystalline subrounded to subangular and subspherical grains, up to 21%, whereas, polycrystalline grains occur in minor amount, reaching a maximum of 2%. Metamorphic lithic fragments represent the most abundant non-carbonate component (NCE) and they mainly prevail in the 20P sample ($Lm_{73}Lss_{26}Lsc_1$). They decrease in the upper 21P sample ($Lm_{14}Lss_{15}Lsc_{71}$). Aphanitic metamorphic lithic fragments include subrounded flattened phyllite, slate and fine-grained micaschist grains. Phaneritic rock fragments of metamorphic rocks, mostly quartz-rich metamorphites and metarenites are also present in large amounts and vary from 4% to 25% (20P sample). Sedimentary lithic fragments comprise siltstone and chert grains (aphanitic), up to 2%, and sandstone grains (phaneritic), represented by quartzoarenite fragments with internal calcite sparitic cement and siliciclastic matrix (14% in 20P sample). Extrabasinal carbonate grains (CE) occur in the overall petrofacies and is more abundant in the 21P sample. It consists of reworked *Nummulites* and *Discocyclina* skeletons, up to 21%, and carbonate lithic fragments, up max to 26% in the sample 18P. These latter constituents include wackestone-mudstone with several biofacies represented by benthic foraminifers, thin-shelled bivalves, radiolarians, *Bryozoans* and *Rodoficean* algae, and shallow-marine clasts comprising ooids, minor oncoids and bivalves. Lepidocyclinid (CI) are also present. Samples of the Rio Pliego petrofacies are poor sorted and several grains have only tangential and minor concavo-convex contacts with neighboring grains, indicating a strong mechanical compaction. Aphanitic metamorphic and sedimentary lithic fragments have undergone initial ductile-brittle deformation. The matrix is mainly made of fine sand and silt-size grains with minor dark brown-reddish clay.

The fine-grained sandstones (22P sample) at the top of the succession are quartzolithic with increased quartz content ($Qm_{76}F_1Lt+CE_{23}$) characterized by a large amount of monocrystalline quartz grains.

The Burdigalian p.p. Depositional Sequence (El Niño Formation) contains fine-medium grained sandstones that are quartzolithic ($Qm_{61}F_0Lt+CE_{39}$; Fig. 6) with significant extrabasinal carbonate grains ($NCE_{64}CI_0CE_{36}$). Quartz grains are the most abundant component whereas tectonics-fabric polycrystalline quartz grains occur in minor amount, up to 4%. Metamorphic lithic fragments, represented by a few slate and phyllite grains, are strongly depleted with respect to the samples of the underlying Rio Pliego Fm. Extrabasinal carbonate content (CE) is composed of bioclasts,

ACCEPTED MANUSCRIPT

including single sand-size angular and broken skeletons of *Nummilites*, *Discocyclinas*, *Bryozoan*, *Rodoficean* algae, bivalve and crinoid fragments, and subrounded to angular carbonate lithic fragments (CE). These fragments consist of bioclastic mudrocks with radiolarians and sponge spicules and shallow-water clasts with grainstone texture including ooids and peloids. Several single calcite spars and undetermined grains replaced by calcite are also present. These sandstones are well sorted. The interstitial component is filled by blocky sparitic calcitic cement and locally by dark brown phyllosilicate matrix.

6. Mineralogical and geochemical composition of the mudrocks

6.1 Mineralogy of the mudrocks

Whole-rock XRD analyses (Tab. 3) show important mineralogical variation for the studied mudrocks (Fig. 8). Quartz is the main mineralogical component in syn-orogenic formations, ranging from 10% to 57% of the bulk rock, whereas calcite is most abundant in pre-orogenic formations with values up to 87%. Dolomite is particularly abundant in the Bosque Fm with values up to 48%. Feldspars (plagioclase and K-feldspar) are minor in the pre-orogenic successions, and occur in large amounts in the Rio Pliego Fm with values up to 23% (16A sample). Hematite is minor and is only present in the Mula Fm (values up to 3%); trace amounts occur also in the Rio Pliego Fm. Phyllosilicates range from trace amounts up to 19% in pre-orogenic successions and from 10% to 44% in the syn-orogenic successions. Illite and micas prevail with values up to 33%, whereas chlorite ranges up to 8% and kaolinite is minor. C–S and I-S mixed layers are only present in trace amounts. Variation of mineral concentrations is related to different source areas that influence the chemical and mineralogical composition of the sediments.

6.2 Whole-rock geochemistry of the mudrocks

Major and trace element concentrations are listed in Table 4. Mudrocks of syn-orogenic successions (in particular El Niño and Rio Pliego formations) are characterized by narrow compositional changes for SiO_2, Al_2O_3, K_2O and CaO, with concentrations fairly close to those of the UCC (Upper Continental Crust; McLennan et al., 2006). Mudrocks of the pre-orogenic successions show a similar composition, with higher concentrations of Ca and Sr than syn-orogenic successions and UCC. All the samples contain very low Na content probably due to the absence of Na-plagioclase. Magnesium is enriched only in the Bosque Fm due to the abundance of dolomite, as shown by the

ACCEPTED MANUSCRIPT

mineralogical analyses. The main variations are related to the Si+Al content as they are higher in the syn-orogenic than the pre-orogenic deposits. The Ca+Mg content is higher in the pre-orogenic than in the syn-orogenic deposits (Fig. 9).

In a ternary plot of SiO_2 (representing quartz or opaline silica), Al_2O_3 (representing mica/clay minerals), and CaO (representing carbonate) (*e.g.*, Wehausen et al., 2003; Perri et al., 2012, 2014), the mudrocks of the pre-orogenic successions plot close to the CaO apex toward the direction of the Al-Si side due to the abundance of carbonate phases. Samples from syn-orogenic formations represent a mixture of an aluminosilicate and carbonate content, which is more evident in the Bosque Fm (Fig. 10). These chemical associations and elemental variations are related to the mineralogical composition of the studied mudrocks, as shown above by the mineralogical analyses.

7. Discussion

7.1 Provenance relations

The heterogeneous composition of the sandstones and rudstones and the mudrock compositional data indicate that the Tertiary studied succession had their multiple source areas derived from metamorphic, siliciclastic and carbonate rocks, with a minor supply of mafic rocks. The siliciclastic sandstones plot mainly in a wide area at the QmLt side in a QmFLt diagram (Fig. 6), reflecting a transition provenance from cratonic and recycled orogenic areas (e.g. Dickinson, 1985). The basement of the Malaguide Complex mainly consists of a pre-Ordovician to Late Carboniferous siliciclastic, siliceous and metasedimentary (slate, phyllite, carbonate and quartzite) succession including thin carbonate lenses and conglomerate bodies with some clasts of silicic plutonic rocks (Vera, 2004). This is overlain by a Late Triassic to Cretaceous carbonate succession composed of peritidal dolostones, ooidal and nodular limestones, thin-bedded mudrocks and cherty mudrocks. Related sedimentary successions also occur in other Alpine–Mediterranean Chains equivalent to the Malaguide Complex, such as the Moroccan Ghomarides, the Algerian Kabylides (Wildi, 1983), or the Italian Calabrian Terranes (Bonardi et al., 2001).

The composition of the pre-orogenic cycle rocks is dominantly composed of carbonate rocks, as seen in both petrographical and mineralogical-geochemical data (Figs. 8 and 9). The occurrence of benthic macro foraminifers, *such* as *Nummulites* and *Discocyclina, Rodoficean* algae, *Bryozoans,* and crinoid fragments suggests a palaeoenvironment of a shallow-marine carbonate ramp. The siliciclastic samples are mature (i.e. Espuña Fm: $Qm_{96}F_0Lt+CE_4$; As Fm: $Qm_{92}F_0Lt+CE_8$) and indicate a clear provenance from a craton interior area. Moreover, the presence of few phaneritic

ACCEPTED MANUSCRIPT

quartz-rich metamorphic lithic fragments suggests the influence of a high-medium grade metamorphic basement, more probably of extra Malaguide origin and may be identifiable with Calabro-Kabilide areas (Martín-Algarra et al., 2000). In the As Formation (Early Oligocene depositional sequence), the reworked macro foraminifers and extrabasinal carbonate lithic fragments demonstrated a detrital supply from uplifted Paleocene and Cuisian-Early Lutetian Depositional sequences of the Morrón de Totana unit (i.e. Mula, Espuña and Valdelaparra Formations).

The beginning of the syn-orogenic cycle (Bosque Fm) is marked by a continuous carbonate debris supply coming from older Malaguide Paleocene-Eocene formations. The subordinate presence of shallow-marine platform lithic fragments including ooidal grainstones also indicates that Mesozoic carbonate bodies of the Malaguide Complex (more probably eroded from the Perona unit which overthrust on the Morrón de Totana unit) began to uplift. In addition, the mudrocks of the Bosque Fm are characterized by a large dolomite content (Fig. 8). These data thus confirm the provenance from Mesozoic rocks, including the Triassic-Jurassic dolostones.

The sharp increase of the siliciclastic component recognized in the Rio Pliego and El Niño Formations suggests abrupt changes of the source area involving the Palaeozoic (or older) to early Mesozoic metamorphic and terrigenous Malaguide rocks close to the Malaguide Complex and neighbor domains. A significant contribution from low-medium grade metamorphic rocks is testified by the abundance of slate, phyllite and metarenite grains in sandstone and the micro conglomerate strata. However, metarenite grains, including disoriented quartz grains with sutural contacts immersed in a phyllosilicate matrix, could be related to an unknown deep Malaguide metamorphic basement (Sánchez Navas et al., 2016) rocks (Precambrian) or to neighbor domains as the Calabro-Kabilide blocks (Martín-Algarra et al., 2000). In the case of the Burdigalin *p.p.* El Niño Fm, an Alpujarride origin could also be evoked for these metamorphic rocks. The presence of sedimentary detritus, represented by quartzo-arenite fragments, indicates an additional source from the Late Triassic arenites that could be comparable with detrital members of the Saladilla Fm (i.e. redbeds; Critelli et al., 2008; Perri et al., 2013). Carbonate grains are also abundant in the Rio Pliego Fm suggesting provenances from uplifted Mesozoic-Cenozoic terrains. Chemical and mineralogical data of the mudrock samples also point towards a similar provenance scenario. In particular, the relative high concentration of barium in some samples of the Rio Pliego Fm indicates that hydrothermal and metasomatic processes could locally play an important role, possibly related to the partial replacement of some rocks as a result of interaction with hydrothermal solutions or other fluids (e.g. Hetherington et al., 2008 and references therein). The high Ba concentration in

ACCEPTED MANUSCRIPT

some samples is probably related to the evaporite and carbonate beds of the Saladilla Fm that was exhumed during the Late Oligocene-Early Miocene syn-orogenic evolution.

High concentrations of Fe, Mg, Cr and Ni, even in stronglu-weathered environments, indicate provenance from mafic or ultramafic rocks (e.g., ophiolitic sources), whereas very low values in them are typical of felsic source(s). In particular, mafic–ultramafic sources tend to have high ferromagnesian abundances and such a provenance would result in increasing Cr/V ratio and decreasing Y/Ni ratio (e.g., Hiscott, 1984; Amendola et al., 2016; Perri et al., 2016a and references therein). Syn-orogenic formations are characterized by higher Cr/V values than pre-orogenic formations (Fig. 11a). In particular, the distribution of some samples of the Rio Pliego and El Niño Formations in Cr vs. Ni diagram confirms a mafic contribution for syn-orogenic samples (Fig. 11b). Such formations probably recorded residual signals of provenance from volcanic or ophiolitic members of an unknown very older Malaguide basement (or to neighbor domains as the Calabro-Kabilide blocks) and an Alpujarride or Alpujarride-Malaguide transitional Units, in the case of the El Niño Fm.

7.2 Sorting and recycling

Mechanical sorting during transport and deposition may affect the chemical composition of terrigeneous sediments and the distribution of certain elements; in particular, these processes fractionate Al_2O_3 (clay minerals) from SiO_2 (quartz and feldspars) and TiO_2 (mostly present in clay minerals and Ti-oxides) from Zr (present in zircon, and sorted with quartz). Thus, a ternary plot based on Al-Ti-Zr illustrates sorting-related fractionations by mixing trends on this diagram (e.g., Garcia et al., 1991; Mongelli et al., 2006; Critelli et al., 2008). The studied samples fall in a trend toward the Zr apex, which could be due to recycling effects (Fig. 12). The effect of sedimentary recycling is more marked in the pre-orogenic cycle where Zr enrichment is mainly recorded. This suggests that the sediments were reworked before deposition through prolonged processes of sedimentary transport and recycling.

7.3 Paleoweathering and paleotectonic features

The degrees of weathering in source areas affect the distribution and abundances of alkali and alkaline-earth elements in fine-grained sediments. The chemical index of alteration (CIA; Nesbitt and Young 1982) together with the A-CN-K (Al_2O_3, CaO^*+Na_2O, K_2O where CaO^* represents Ca in silicate minerals only) are commonly used to quantify the degree of source-area weathering. Both

ACCEPTED MANUSCRIPT

the CIA and the CIA´, expressed as molar volumes of [Al/(Al+Na+K)]×100 and, thus, calculated without the CaO content (e.g., Perri et al., 2012, 2014, 2015; Amendola et al., 2016), have been used in this study.

The studied mudrocks have low-moderate CIA values and high variability of the CIA index (from 53 to 69 for the pre-orogenic cycle; from 54 to 71 for the syn-orogenic cycle). In the A-CN-K diagram the samples plot in a wide group following a trend from the CN apex towards the illite-muscovite point of the A-K join (Fig. 13a). This trend indicates a source area with low-moderate weathering in non-steady-state conditions that changed from the pre-orogenic to the syn-orogenic cycle. Furthermore, the samples are characterized by CIA´ values (average CIA´=75 for the pre-orogenic cycle; average CIA´=71 for the syn-orogenic cycle) similar to the CIA values, also testifying low to moderate paleoweathering conditions, with a distribution of the samples in the A-N-K diagram (Fig. 13b) along the A-K join toward the K apex suggesting K-enrichment during diagenesis.

In particular, the pattern described in the A-CN-K diagram is typical of a source area where active tectonism allows erosion of all zones within weathering profiles developed on source rocks (e.g., Nesbitt et al., 1997). The geodynamic evolution of the Sierra Espuña area is characterized by uplift and erosional processes during the transition from the pre-orogenic to syn-orogenic cycle due to the active tectonism of the studied area in the Late Oligocene-Early Miocene period, as shown below (Fig. 14).

8. Palaeogeographical implications and conclusions

The Cenozoic time span is characterized by seasonal climate condition that initially favored recycling processes. The tectonic evolution of the Malaguide Complex, particularly in the Sierra Espuña area, is very complex and is marked by different structural stages (Martín-Martín et al., 2006a; Martín-Rojas et al., 2007) that strongly influenced the composition, sorting and transport of clastic debris deposited in the Mula-Pliego basin. This period was also the time of convergence between the Internal Betic Units, belonging to the western and southern margin of the Mesomediterranean Microplate, and the External Betic Units, belonging to the Iberian plate. Such convergence led to the break-up of the Mesomediterranean Microplate with the progressive closure of the Nevado-Filabride oceanic basin westward and northward, and the consequent opening of Western Mediterranean basins (i.e. Alboran, Balearian, Argerian, Provençal basins: e.g., Guerrera et al., 1993, 2005; Perrone et al., 2006; Critelli et al., 2008; Perri et al., 2013). The final collision formed the present Betic Cordillera. The convergence started in the Latest Cretaceous, and

ACCEPTED MANUSCRIPT

progressed rapidly till the latest Eocene-earliest Oligocene with the superposition of the Malaguide Complex onto the Alpujarride Complex (Martín-Martín et al., 2006a; Martín-Rojas et al., 2007 and references therein). Afterwards, in the Late Oligocene, a second superposition stage took place with the upper Malaguide unit (Perona Unit) being superposed over the Morron de Totana Unit (Fig. 14), generating related structures located at north of the Sierra Espuña (i.e. the Espuña fold). During the westward displacement of the Internal Betic Zone and collision against the External Zones during the Burdigalian some authors have proposed rotations of the units located along the Internal–External Zone contact for the Betic Cordillera and the Rif (Durand-Delga, 1972; Platzman et al., 1993; Sanz de Galdeano, 1997; Platzman and Platt., 2004; Platt et al., 2003; 2013), and in particular in the area of the Sierra Espuña (Allerton et al., 1992 and 1993; Martín-Martín et al., 2006a).

This geodynamic evolution is characterized by the first evidence of the extrabasinal detrital supplies recorded in the Early Oligocene Depositional Sequence. Such fragments were derived from the former basement cover of the Morron de Totana Unit, that were more probably exhumed as a consequence of the initial superposition of the Perona Unit over the Morron de Totana Unit (Fig. 14). Such superposition is more marked starting from the beginning of the syn-orogenic cycle in the Late Oligocene-to-Aquitanian. In the Bosque depositional area the first appearance of the Mesozoic carbonate fragments highlights the sedimentary contribution from the lower portion of the Perona Unit that was exhumed as response of the increasing of tectonic superposition. Therefore the uplift of the Mesozoic limestones enhanced the overflowing of shallow-marine carbonate debris toward West. Such a carbonate supply is mixed with that derived from the Tertiary depositional sequences of the Morron de Totana Unit. In the Rio Pliego Fm the large amount of metamorphic and recycling siliciclastic lithic fragments indicate a clear provenance from the Paleozoic basement of the Morron de Totana Unit that was exhumed in the northern part of the Mula-Pliego basin and related to the successive convergence of the IBZ against more external domains (Fig. 14). The mixed metamorphic and sedimentary lithic fragmensts overflowed in the opposite direction with respect to the carbonate supplies of the As and Bosque formations (Fig. 14). The slight mafic supply recorded in the mudrocks of the Rio Pliego and El Niño formations could be explained by the uplift of an unknown metamorphic Malaguide basement, and in the case of the El Niño Fm, from extra-Malaguide units (i.e. Alpujarrides or transitional Alpujarride-Malaguide ones) exhumed before the successive collision of the IBZ with the EBZ. Furthermore, mafic signals could be also a result of erosion from exhumed Triassic Malaguide vulcanites.

The provenance from a multi-source area, marked by exhumation of the Malaguide basement and lower units of the IBZ, is suggested by the very heterogeneous composition of the pre-orogenic and

ACCEPTED MANUSCRIPT

syn-orogenic deposits. The paleoweathering suggest a source area with low-moderate weathering in non-steady-state conditions that changed from the pre-orogenic to the syn-orogenic cycle. These indices further suggest a source area characterized by active tectonism that allows erosion of all zones within weathering profiles developed on source rocks, due to the uplift and erosional processes during the transition from the pre-orogenic to syn-orogenic cycle. The mineralogical composition of the studied deposits characterized by high concentrations of kaolinite and chlorite, representing overall warmer and more humid conditions, for syn-orogenic than for pre-orogenic deposits, and suggests different paleoclimatic conditions during the transition from the Paleocene-Early Oligocene to Late Oligocene-Early Miocene.

The studied area due to the thickness, outcrop quality and continuity of the Cenozoic succession is crucial for the correlation among the "internal zones" of other Circum-Mediterranean belts (Rif, Tell, Calabria-Peloritani Arc, Apennines, etc). The data, discussion and conclusions obtained here are of great interests giving constraints for future studies in the western Tethyan area.

Acknowledgements

Support from Ministero Italiano dell'Università e della Ricerca Scientifica to S. Critelli, an Università della Calabria Erasmus Placement grant to S. Montone, and a CARICAL Foundation grant to U. Amendola, are acknowledged. CGL2016-75679-P research projects (Spanish Ministry of Education and Science) and by Research Groups and projects of the Generalitat Valenciana from Alicante University (CTMA-IGA) are also acknowledged. The authors are indebted to Robert Cullers, Agustín Martín-Algarra and the editor David J Bottjer for their reviews, discussions and suggestions on the manuscript.

ACCEPTED MANUSCRIPT

ACCEPTED MANUSCRIPT

References

Alcalá, F., Guerrera, F., Martín-Martín, M., Raffaelli, G., Serrano, F., 2013. Geodynamic implications derived from Numidian-like distal durbidites deposited along the Internal-External Domain Boundary of the Betic Cordillera (S Spain). Terra Nova 2, 119-129.

Allerton, S., Platt, J. P., Platzmann, E. S., McClelland, E., Lonergan, L., 1992. Paleomagnetic study of Tectonic Rotations in the Eastern Betic Cordillera, Southern Spain. M.L. and M. Calvo (Eds.), Física de la Tierra. Paleomagnetismo y Tectónica en las Cordilleras Béticas. Ed. Complutense. Madrid, pp. 185-204.

Allerton, S., Lonergan, L., Platt, J. P., Platzmann, E. S., and McClelland, E. (1993). Palaeomagnetic rotations in the eastern Betic Cordillera, southern Spain. Earth Plan. Sci. Lett. 199, 225-241.

Amendola, U., Perri, F., Critelli, S., Monaco, P., Cirilli, S., Trecci, T., Rettori R., 2016. Composition and provenance of the Macigno Formation (Late Oligocene-Early Miocene) in the Trasimeno Lake area (northern Apennines). Mar. Petr. Geol. 69, 146-167.

Arribas, M.E., Estrada, R., Obrador, A., Rampone, G., 1996. Ditribución y ordenación de Microcodium en la Formación Tremp: anticlinal de Campllong (Pirineos orientales, provincial de Barcelona). Rev. Soc. Geol. España. 9, 1-2.

Baccelle, L., Bosellini, A., 1965. Diagrammi per la stima visiva della composizione percentuale nelle rocce sedimentarie. Annali Università di Ferrara Sez. IX Scienze Geologiche e Paleontologiche 1, 59-62.

Bonardi, G., Cavazza, W., Perrone, V., Rossi, S., 2001. Calabria-Peloritani Terrane and Northern Ionian Sea, in: Vai, G.B., Martini I.P. (Eds.), Anatomy of an Orogen: The Apennines and Adjacent Mediterranean Basins. Kluwer Academic Publishers, Dordrecht, pp. 287–306.

Bouillin, J.P., 1986. Le bassin maghrébin : une ancienne limite entre l'Europe et l'Afrique à l'ouest des Alpes. Bull. Soc. Geol. Fr., (8), II, 4, 547–558.

Caracuel, J., Sandoval, J., Martín-Martín, M., Estévez-Rubio, A., Martín-Rojas, I., 2006. Jurassic biostratigraphy and paleoenvironmental evolution of the Malaguide complex from Sierra Espuña (Internal Betic Zone, SE Spain). Geobios 39, 25-42.

Cavalcante, F., Fiore, S., Lettino, A., Piccarret, G., Tateo, F., 2007. Illite–smective mixed layers in sicilide shales and piggy-back deposits of the Gorgoglione Formation (Southern Apennines): geological inferences geodynamic implications. Boll. Soc. Geol. It. 126, 241–254.

Cecca, F., Critelli, S., De Capoa, P., Di Staso, A., Giardino, S., Messina, A., Perrone V., 2002. Nouvelle datation et interprétation de la succession sédimentaire de Fiumara Sant'Angelo

ACCEPTED MANUSCRIPT

(Monts Péloritains; Italie méridionale): conséquences pour la paléogéographie mésozoique de la Méditerranée centrale. Bull. Soc. Géol. Fr. 173, 2, 171-184.

Critelli, S., Ingersoll, R.V., 1995. Interpretation of neovolcanic versus palaeovolcanic sand grains: an example from Miocene deep-marine sandstone of the Topanga Group (southern California). Sedimentology 42, 783–804.

Critelli, S., Le Pera, E., 1994. Detrital modes and provenance of Miocene sandstones and modern sands of the Southern Apennines thrust-top basins (Italy). J. Sed. Res. 64, 824–835.

Critelli, S., Le Pera, E., Galluzzo, F., Milli, S., Moscatelli, M., Perrotta, S., Santantonio, M., 2007. Interpreting siliciclastic-carbonate detrital modes in Foreland Basin Systems: an example from Upper Miocene arenites of the Central Apennines, Italy, in: Arribas J., Critelli S. and Johnsson M. (Eds.), Sedimentary Provenance: Petrographic and Geochemical Perspectives. Geological Society of America Special Paper 420, pp. 107-133.

Critelli, S., Mongelli, G., Perri, F., Martín-Algarra, A., Martín-Martín, M., Perrone, V., Dominici R., Sonnino M., Zaghloul, M.N., 2008. Compositional and geochemical signatures for the sedimentary evolution of the Middle Triassic–Lower Jurassic continental redbeds from Western-Central Mediterranean Alpine Chains. J. Geol. 116, 375–386.

Dickinson, W.R., 1985. Interpreting provenance relations from detrital modes of sandstones, in: Zuffa, G.G. (Ed.), Provenance of Arenites. Nato ASI series, 148, D. Reidel Pub. Co., Dordrecht, The Netherlands, pp. 333–361.

Dickinson, W.R., 1970. Interpreting detrital modes of graywacke and arkose. J. Sed. Petrol. 40, 695–707.

Dunham, R. J., 1962. Classification of carbonate rocks according to depositional texture, in: Ham, W. E. (Ed.), Classification of carbonate rocks: American Association of Petroleum Geologists Memoir, pp. 108-121.

Durand-Delga, M., 1972. La courbure de Gibraltar, extrémité occidentale des chaînes alpines, unit l'Europe et l'Afrique. Eclogae geol. Helv. 65, 267-278.

El Talibi, H., Zaghloul, M.N., Perri, F., Aboumaria, K., Rossi, A., El Moussaoui, S., 2014. Sedimentary evolution of the siliciclastic Aptian–Albian Massylian flysch of the Chouamat Nappe (central Rif, Morocco). J. Afr. Earth Sci. 100, 554-568.

Embry, A.F., Klovan, J.E., 1971. A Late Devonian reef tract on Northeastern Banks Island, NWT. Bull. Can. Petrol. Geol. 19, 730-781.

García, D., Coehlo, J., Perrin, M., 1991. Fractionation between TiO_2 and Zr as a measure of sorting within shale and sandstone series (northern Portugal). Eur. J. Miner. 3, 401–414.

ACCEPTED MANUSCRIPT

Gazzi, P., 1966. Le arenarie del Flysch sopracretaceo dell'Appennino modenese; correlazioni con il Flysch di Monghidoro. Miner. Petr. Acta 12, 69–97.

Guerrera, F., Martín-Algarra, A., Perrone, V., 1993. Late Oligocene–Miocene syn-late-orogenic successions in western and central Mediterranean chains from the Betic cordillera to the southern Apennines. Terra Nova 5, 525–544.

Guerrera, F., Martin-Martin, M., Perrone, V., Tramontana, M., 2005. Tectono-sedimentary evolution of the southern branch of western thetys (Maghrebian Flysch Basin and Lucanian Ocean) on the basis of the stratigraphic record. Terra Nova 17, 358–367.

Guerrera, F., Martín-Algarra, A., Martín-Martín M., 2012. Tectono-sedimentary evolution of the "Numidian Formation" and Lateral Facies (southern branch of the western Tethys: constraints for central-western Mediterranean geodynamics. Terra Nova. 24, 3-41.

Guerrera, F., Martín-Martín, 2014. Geodynamic events reconstructed in the Betic, Maghrebian and Apennine chains (central-western Tethys). Bull. Soc. geol. France. 185/5, 329-341.

Guerrera, F., Martín-Martín, M., Raffaelli, G., Tramontana, M., 2015. The Early Miocene "Bisciaro volcaniclastic event" (northern Apennines, Italy): a key study for the geodynamic evolution of the central-western Mediterranean. Int. J. Earth Sci. 104, 1083-1106.

Hetherington, C.J., Lundmark, M., Graeser, S., Gierè, R., 2008. The chemistry of barium anomalies in the Berisal Complex, Simplon Region, Switzerland. Int. J. Earth Sci. 97, 51–69.

Hiscott, R.N., 1984. Ophiolitic source rocks for Taconic-age flysch: trace element evidence. Geol. Soc. Am. Bull. 95, 1261-1267.

Ingersoll, R.V., Bullard, T.F., Ford, R.L., Grimm, J.P., Pickle, J.D., Sares, S.W., 1984. The effect of grain size on detrital modes: a test of the Gazzi–Dickinson point-counting method. J. Sed. Petrol. 54, 103–116.

Ingersoll, R.V., Suczek, C.A., 1979. Petrology and provenance of Neogene Sand from Nicobar and Bengal fans, DSDP sites 211 and 218. J. Sed. Petrol. 49, 1217–1228.

Krumm, S., 1996. WINFIT 1.2 - version of November (1996), (The Erlangen geological and mineralogical software collection) of WINFIT 1.0: a public domain program for interactive profile-analysis under WINDOWS. XIII Conference on Clay Mineralogy and Petrology, Praha, 1994. Acta Univ. Carolinae Geol. 38, 253-261.

Martín-Algarra, A., 1987. Evolución geológica alpina del contacto entre las Zonas Internas y la Zonas Externas de la Cordillera Bética. Tesis Univ. Granada. 1171 pp.

Martín-Algarra, A., Messina, A., Perrone, V., Russo, S., Maate, A., Martín-Martín, M., 2000. A Lost Realm in the Internal Domains of the Betic-Rif Orogen (Spain and Morocco):

ACCEPTED MANUSCRIPT

Evidence from Conglomerates and Consequences for Alpine Geodynamic Evolution. J Geol. 108, 447-467.

Martín-Martín, M., Martín-Algarra, A., 2002. Thrust sequence and syntectonic sedimentation in a piggy-back basin: the Oligo-Aquitanian Mula-Pliego Basin (Internal Betic Zone, SE Spain). C. R. Geosci. 334, 63-370.

Martín-Martín, M., El Mamoune, B., Martín-Algarra, A., Martín-Pérez, J.A., Serra-Kiel, J., 1997a. Timing of deformation in the Malaguide Complex of the Sierra Espuña (SE Spain). Geodynamic evolution of the Internal Betic Zone. Geol. Mijn. 75, 309-316.

Martín-Martín, M., Martín-Algarra, A., Serra-Kiel, J., 1997b. El Terciario del dominio Maláguide en Sierra Espuña (prov. de Murcia, SE de España. Rev. Soc. Geol. España. 10 (3-4), 265-280.

Martín-Martín, M., El Mamoune, B., Martín-Algarra, A., Serra-Kiel, J., 1997c. La formation As, date de l'Oligocène, est impliquée dans les charriages des unités malaguides supérieures de la Sierra Espuña (zones internes bétiques, province de Murcie, Espagne. C. R. Geosci. 325, 861-868.

Martín-Martín, M., Sanz de Galdeano, C., García-Tortosa, F.J., Martín-Rojas, I., 2006a. Tectonic units from the Sierra Espuña-Mula area (SE Spain): implication on the triassic paleogeography and the geodynamic evolution for the betic-rif internal zone. Geodin. Acta 19/1, 1-9.

Martín-Martín, M., Martín-Rojas, I., Caracuel, J., Estévez-Rubio, A., Martín-Algarra, A., Sandoval, J., 2006b. Tectonic framework and extensional pattern of the Malaguide Complex from Sierra Espuña (Internal Betic Zone) during Jurassic-Cretaceous: implications for the Westernmost Tethys geodynamic evolution. Int. J. Earth Sci. 95, 815-826.

Martín-Martín, M., Serra-Kiel, J., El Mamoune, B., Martín-Algarra, A., Serrano F., 1998. Le Paléocène des Malaguides orientales (Cordillères bétiques, Espagne): stratigraphie et paléogéographie. C. R. Geosci. 326, 35-41.

Martín-Rojas I., Sanz de Galdeano C., Martín-Martín, M. and García-Tortosa F.J. (2007): Geometry and kinematics of an antiformal stack deduced from brittle structures. Example of the Internal Betic Zone in the Sierra Espuña (province of Murcia, Spain). C. R. Geosci. 339, 506-515.

McLennan, S.M., Taylor, S.R., Hemming, S.R., 2006. Composition, differentiation, and evolution of continental crust: constrains from sedimentary rocks and heat flow, in: Brown, M., Rushmer, T. (Eds.), Evolution and Differentiation of the Continental Crust. Cambridge University Press, pp. 92–134.

ACCEPTED MANUSCRIPT

Mongelli, G., Critelli, S., Perri, F., Sonnino, M., Perrone, V., 2006. Sedimentary recycling, provenance and paleoweathering from chemistry and mineralogy of Mesozoic continental redbed mudrocks, Peloritani Mountains, Southern Italy. Geochem. J. 40, 197–209.

Nesbitt, H. W., Young G. M., 1982. Early Proterozoic Climates and Plate Motions Inferred from Major Elements Chemistry of Lutites. Nature 299. 715-717.

Nesbitt H.W., Fedo C.M., Young G.M., 1997. Quartz and feldspar stability, steady and non-steady-state weathering and petrogenesis of siliciclastic sands and muds. J. Geol. 105, 173–191.

Paquet, J., 1969. Étude géologique de l'Ouest de la province de Murcia (Espagne). Mém. du Bureau de Recherches Géol. Min., Paris 48, 1–270.

Perri, F., 2014. Composition, provenance and source weathering of Mesozoic sandstones from Western-Central Mediterranean Alpine Chains. J. Afr. Earth Sci. 91, 32-43.

Perri, F., Critelli, S., Dominici, R., Muto, F., Tripodi, V., Ceramicola, S., 2012. Provenance and accommodation pathways of late Quaternary sediments in the deep-water northern Ionian Basin, southern Italy. Sed. Geol. 280, 244-259.

Perri, F., Critelli, F., Martín-Algarra, A., Martín-Martín, M., Perrone, E., Mongelli, G., Zattin, M., 2013. Triassic redbeds in the Malaguide Complex (Betic Cordillera – Spain): petrography, geochemistry and geodynamic implications. Earth-Sci. Rev. 117, 1-28.

Perri, F., Ohta T., (2014) – Paleoclimatic conditions and paleoweathering processes on Mesozoic continental redbeds from Western-Central Mediterranean Alpine Chains. Palaeogeo., Palaeoclim., Palaeoeco. 395, 144–157.

Perri, F., Borrelli, L., Critelli, S., Gullà, G., 2014. Chemical and minero-petrographic features of Plio-Pleistocene fine-grained sediments in Calabria (southern Italy). Ital. J. Geosci. 133, 101-115.

Perri, F., Dominici, R., Critelli, S., 2015. Stratigraphy, composition and provenance of argillaceous marls from the Calcare di Base Formation, Rossano Basin (northeastern Calabria). Geol. Mag. 152, 193-209.

Perri, F., Caracciolo, L., Cavalcante, F., Corrado, S., Critelli, S., Muto, F., Dominici, R., 2016a. Sedimentary and thermal evolution of the Eocene-Oligocene mudrocks from the southwestern Thrace Basin (NE Greece). Basin Research 28, 319-339.

Perri, F., Critelli, S., Martín-Martín, M., Amendola, U., Montone, S., 2016b. Compositional signatures of the Cenozoic sedimentary successions of the Malaguide Complex (Betic Cordillera, Spain). Rend. Online Soc. Geol. It. 38, 77-80.

Perrone, V., Martín-Algarra, A., Critelli, S., Decandia, F. A ., D'errico, M., Estevez, A., Iannace, A., Lazzarotto, A., Martín-Martín, M., Martín-Rojas, I., Mazzoli, S., Messina, A.,

ACCEPTED MANUSCRIPT

Mongelli, G., Vitale, S., Zaghloul, N. M., 2006. "Verrucano" and "Pseudoverrucano" in the central-western Mediterranean Alpine chains, in: Chalouan, A., Moratti, G., (Eds.), Geology and Active Tectonics of the Western Mediterranean Region and North Africa. Geological Society of London Special Publication 262, pp. 1-43.

Platt, J.P., Allerton, S., Kirker, A., Mandeville, C., 2003. The ultimate arc: differential displacement, oroclinal bending and vertical axis rotation in the Esternal Betic-Rif arc. Tectonics 22 (3), 1017-1029.

Platt, J.P., Behr, W.M., Johanesen, K., Williams, J.R., 2013. The Betic-Rif Arc and Its Orogenic Hinterland: A Review. Annu. Rev. Earth Planet. Sci. 41,14.1–14.45.

Platzman, E.S., Platt, J.P., Olivier, P., 1993. Palaeomagnetic rotations and fault kinematics in the Rif arc of Morocco. J. Geol. Soc. London 150, 707-718.

Platzman, E. S., Platt, J. P., 2004. Kinematics of a twisted core complex: Oblique axis rotation in an extended terrane (Betic Cordillera, southern Spain). Tectonics 23, TC6010.

Sánchez-Navas, A., de Cassia Oliveira-Barbosa, R., García-Casco, A., Martín-Algarra A., 2002. Transformation of Andalusite to Kyanite in the Alpujarride Complex (Betic Cordillera, Southern Spain): Geologic Implications. J. Geol. 120, 557-574.

Sánchez-Navas, A., García-Casco, A., Martín-Algarra, A., 2014. Pre-Alpine discordant granitic dikes in the metamorphic core of the Betic Cordillera: Tectonic implications. Terra Nova, 26, 477-486.

Sánchez-Navas, A., Macaione, E., de Cassia Oliveira-Barbosa, R., Messina, A., Martín-Algarra, A., 2014. Transformation of kyanite to andalusite in the Benamocarra Unit (Betic Cordillera, S. Spain). Kinetics and petrological significance. Eur. J. Min. 28, 337-353.

Sanz de Galdeano, C., 1997. La Zona Interna Bético-Rifeña. Monografías del Sur. Ed. Universidad de Granada, 316 pp.

Serra-Kiel, J., Martín-Martín, M., El Mamoune, B., Martín-Algarra, A., Martín-Pérez, J.A., Tosquella, J., Ferràndez-Cañadell, C.. Serrano F., 1998. Bioestratigrafía y litoestratigrafía del Paleógeno del area de Sierra Espuña (Cordillera Bética oriental, SE de España). Acta Geol. Hispánica. 31 (1-3), 161-189.

Tent-Manclús, J.E., Martín-Martín, M., Martín-Pérez, J.A., Serrano F., 2001. Structural evolution of the Early Miocene in the eastern Betic internal-external zone boundary (SE Spain). Bull. Soc. Geol. France. 172/1, 41-47.

Vera, J.A., 2004. Geología de España. SGE-IGME, Madrid.

ACCEPTED MANUSCRIPT

Wehausen, R., Tian, J., Brumsack, H.-J., Cheng, X., and Wang, P., 2003. Geochemistry of Pliocene sediments from ODP Site 1143 (southern South China Sea), in: Prell, W.L., Wang, P., Blum, P., Rea, D.K., Clemens, S.C. (Eds.), Proc. ODP, Sci. Results, 184, 1–25.

Wildi, W., 1983. La chaîne tello-rifaine (Algérie, Maroc, Tunisie): structure, stratigraphie et évolution du Trias au Miocène. Rev. Géogr. Phys. Géol. Dyn. 24, 201–297.

Zuffa, G. G., 1980. Hybrid arenites; Their composition and classification. J. Sed. Petrol. 50, 21-29.

Zuffa, G.G., 1985. Optical analysis of arenites: influence of methodology on compositional results, in: Zuffa, G.G. (Ed.), Provenance of Arenites. D. Reidel, Dordrecht, pp. 165–189.

ACCEPTED MANUSCRIPT

ACCEPTED MANUSCRIPT

Figure captions

Fig. 1 - A) The Internal Zones of others alpine chains of the Circum-Mediterranean belts (i.e. Rif, Tell, Calabria-Peloritani and Apennine chains). B) Geological sketch map of the Betic Cordillera. C) The Murcia province in SE Spain. D) Paleogeographic reconstruction of the central-western Mediterranean area showing the position of the Mesomediterranean Microplate. Modified from Martín-Algarra (1987), Guerrera et al. (1993, 2005), Perrone et al. (2006), Critelli et al. (2008), Perri et al. (2013).

Fig. 2 - Geological sketch map and cross sections of the study area including the Sierra Espuña *s.s.* and the Mula-Pliego Basin (modified from Martín-Martín and Martín-Algarra, 2002; Martín-Martín et al., 2006a; Martín-Rojas et al., 2007).

Fig. 3 - A, Panoramic view from the northern side the Sierra Espuña; B, shallow marine silts with limestones and calcarenites from the Mula Fm; C, sandy limestones from the Espuña Fm; D, calcarenites and sandy marls with oversized larger foraminifera from the Malvariche Fm; E, shallow-water calcarenites with rounded quartz pebbles As Fm; F, calcarenites and marls from the Bosque Fm; G, micaceous silty marls with turbiditic sandstones and polygenic conglomerates from the Río Pliego Fm; H, siliceous pelites and silexites from the El Niño Fm.

Fig. 4 - Schematic stratigraphy with the studied stratigraphic formations and the related sandstone and mudrock samples.

Fig. 5 - Synthetic stratigraphic column from the Upper Cretaceous-Tertiary succession from the Morrón de Totana Unit of Sierra Espuña (Murcia province, SE Spain).

Fig. 6 - NCE-CI-CE, Qm-F-Lt+CE, Qt-F-L Lm-Lss-Lsc(CE), Rg-Rs+CE-Rm, Rm-CE-Rss triangular plots (according to Dickinson, 1970; Ingersoll and Suczek, 1979; Critelli and Le Pera, 1994; Folk, 1968; Graham et al., 1976) for the studied sandstones. NCE (non-carbonate extrabasinal grains), CI (carbonate intrabasinal grains), CE (carbonate extrabasinal grains), Qm (monocrystalline quartz), F (feldspars), Lt (total lithic fragments), Qt (total quartz grains), L (aphanitic lithic fragments), Lm (metamorphic lithic fragments), Lss (siliciclastic sedimentary lithic fragments), Lsc (carbonate sedimentary lithic fragments), Rg (plutonic rock fragments), Rm (metamorphic rock fragments), Rs (sedimentary rock fragments), Rss (siliciclastic sedimentary rock fragments).

Fig. 7 - Photomicrographs of sandstones of the Cenozoic Malaguide formations. A, Espuña Fm (sample 4P); B, Malvariche Fm (sample 7P); C, Bosque Fm (15P); D: As Fm (13P); E-F, Río Pliego Fm (samples 18P and 19P).

Fig. 8 - Mineralogical variations along the studied formations.

Fig. 9 - Major elements (SiO_2+Al_2O_3 and CaO+MgO) variations along the studied formations.

ACCEPTED MANUSCRIPT

Fig. 10 - Ternary plot showing the relative proportions of Al_2O_3 (representing mica/clay minerals), SiO_2 (representing quartz) and CaO (representing carbonate) of the studied mudrock samples.

Fig. 11 - Provenance diagrams based on (a) Cr/V vs. Y/Ni relationships (after Hiscott, 1984) and (b) Cr vs. Ni ratios.

Fig. 12 - Ternary plot based on the relative proportions of $15*Al_2O_3$, $300*TiO_2$ and Zr (after García et al., 1994) of the studied mudrock samples.

Fig. 13 – (A) Ternary A-CN-K plot (Nesbitt and Young, 1982) and (B) A-N-K plot (Perri et al., 2012, 2014, 2015; Amendola et al., 2016) plots. Key: A, Al_2O_3; C, CaO; N, Na_2O; K, K_2O; Kln, kaolinite; Chl, chlorite; Gbs, gibbsite; Gr, granite; Ms, muscovite; Ilt, illite; Smt, smectite; Plg, plagioclase; Kfs, K-feldspar; Bt, biotite.

Fig. 14 - Paleogeographic and geodynamic evolutionary model for the Sierra Espuña area from the Paleocene to the Serravallian.

ACCEPTED MANUSCRIPT

ACCEPTED MANUSCRIPT

Table captions

Tab. 1 -Raw point-count data of the studied sandstones.

Tab. 2 - Recalculated modal point-count data of the studied sandstones.

Tab. 3 - Mineralogical composition of the studied mudrocks.

Tab. 4 - Chemical composition and ratios of the studied mudrocks.

ACCEPTED MANUSCRIPT

ACCEPTED MANUSCRIPT

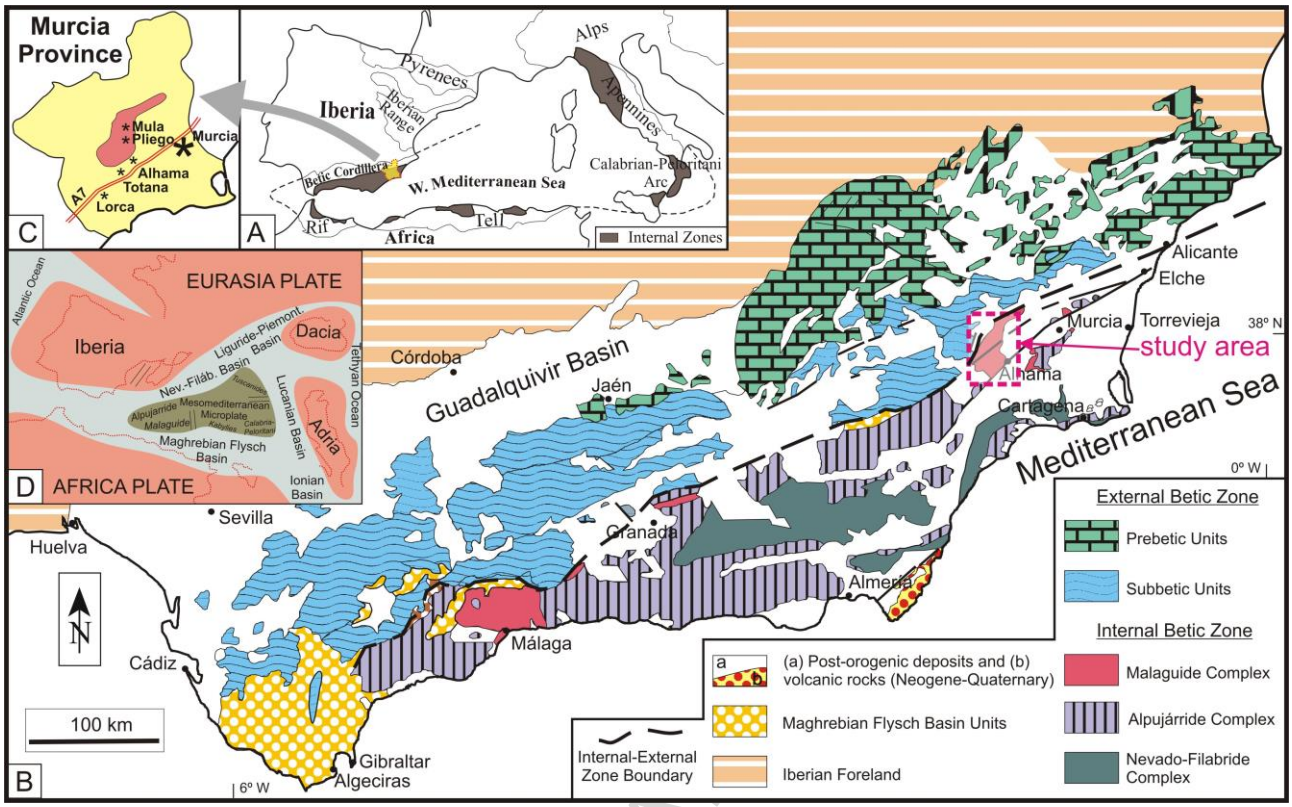

Figure 1

ACCEPTED MANUSCRIPT

ACCEPTED MANUSCRIPT

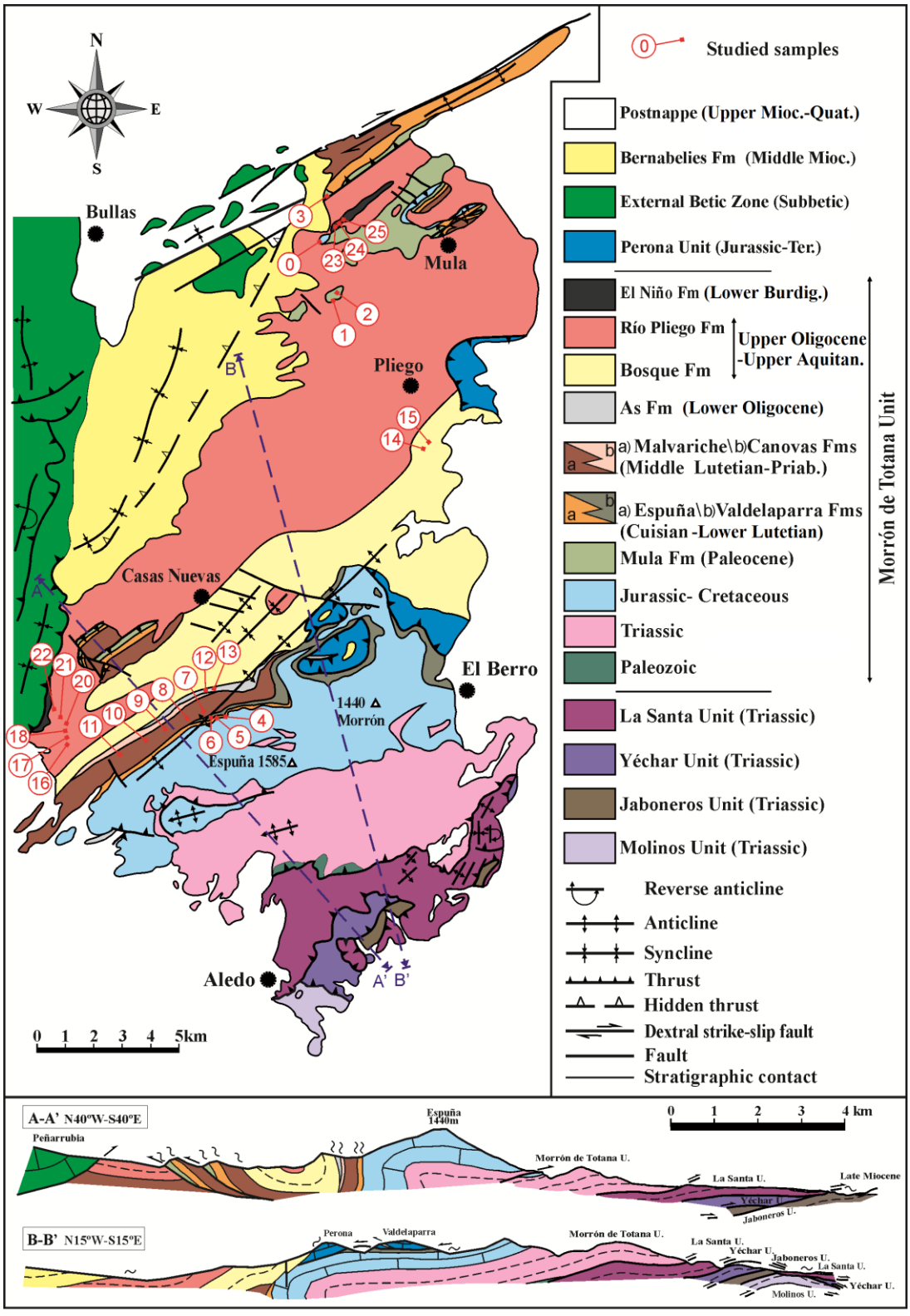

Figure 2

ACCEPTED MANUSCRIPT

Figure 3

ACCEPTED MANUSCRIPT

Sedimentary Cycle	Depositional Sequence	Studied Formation	Sandstones samples	Mudrocks samples
Lower Miocene Upper Oligocene (syn-orogenic)	Lower-Middle Burdigalian	El Niño Fm	23P-24P-25P	23A-24A-25A
	Upper Aquitanian Chattian	Río Pliego Fm / Bosque Fm	16P-17P-18P 19P-20P-21P -22P 14P-15P	16A-17A-18A 19A-20A-21A -22A 14A-15A
Lower Oligocene Paleocene (pre-orogenic)	Lower Rupelian	As Fm	12P-13P	12A-13A
	Priabonian Middle Lutetian	Cánovas Fm / Malvariche Fm	7P-8P-9P 10P-11P	7A-8A-9A 10A-11A
	Lower Lutetian Cuisian	Valdelaparra Fm / Espuña Fm	4P-5P-6P	4A-5A-6A
	Paleocene	Mula Fm	1P-2P-3P	1A-2A-3A

Figure 4

ACCEPTED MANUSCRIPT

ACCEPTED MANUSCRIPT

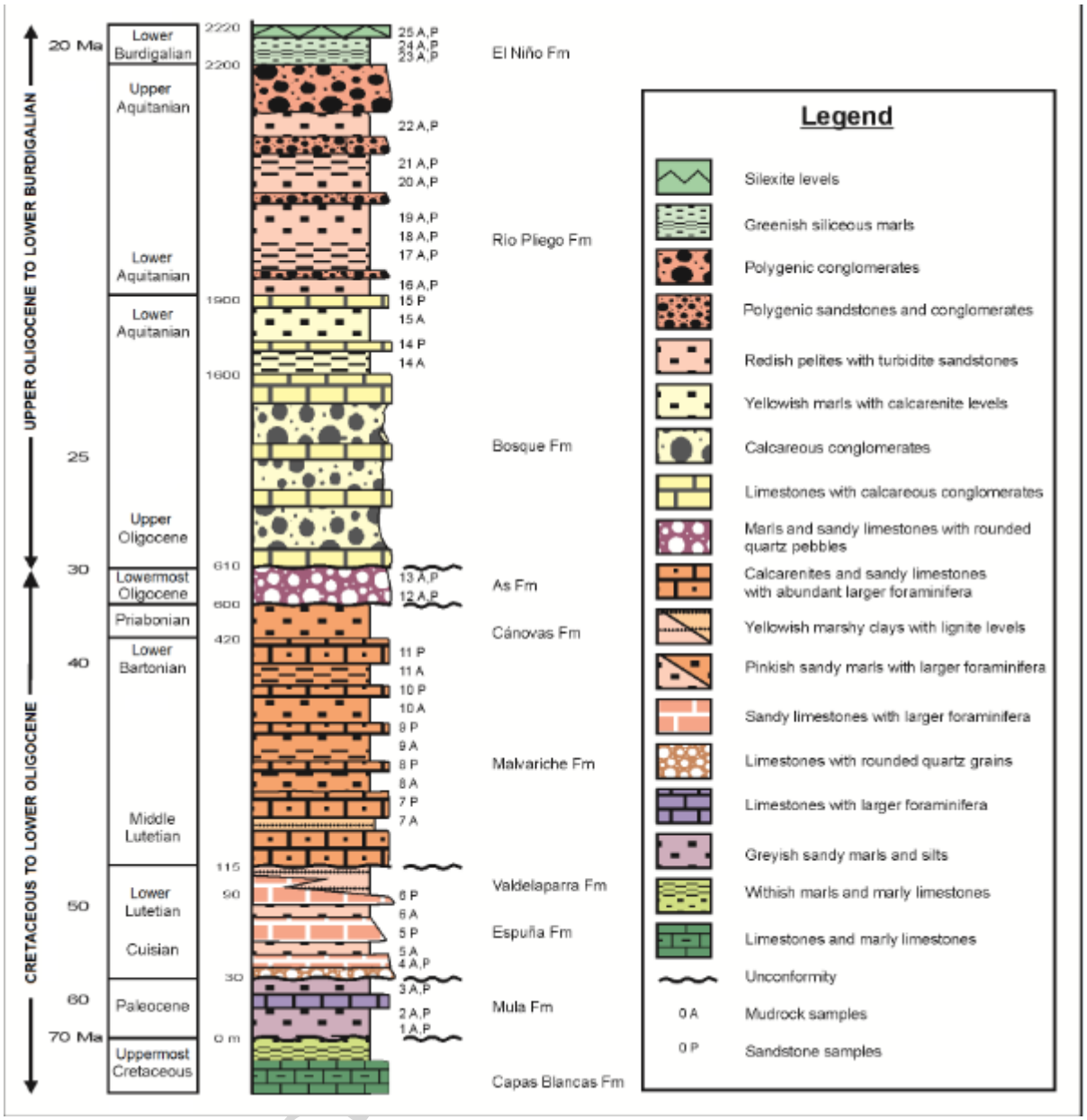

Figure 5

ACCEPTED MANUSCRIPT

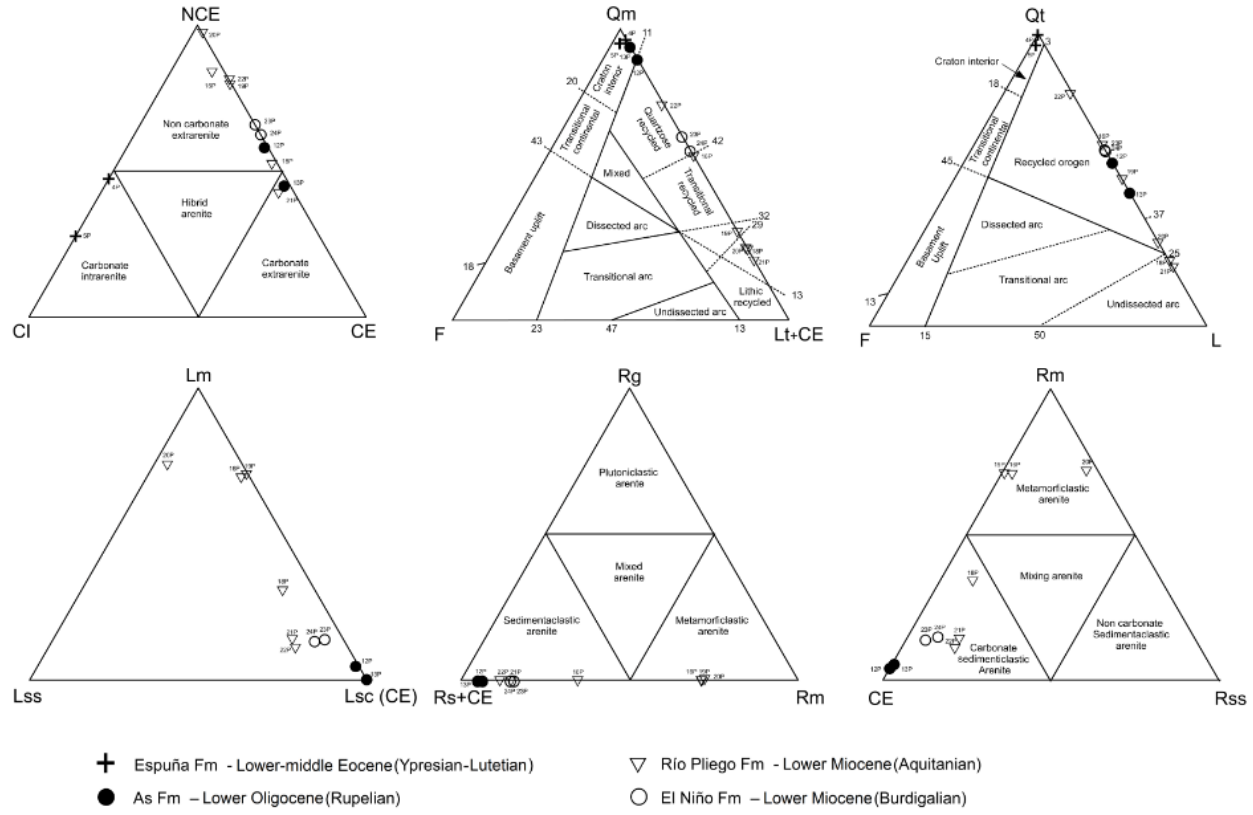

Figure 6

ACCEPTED MANUSCRIPT

ACCEPTED MANUSCRIPT

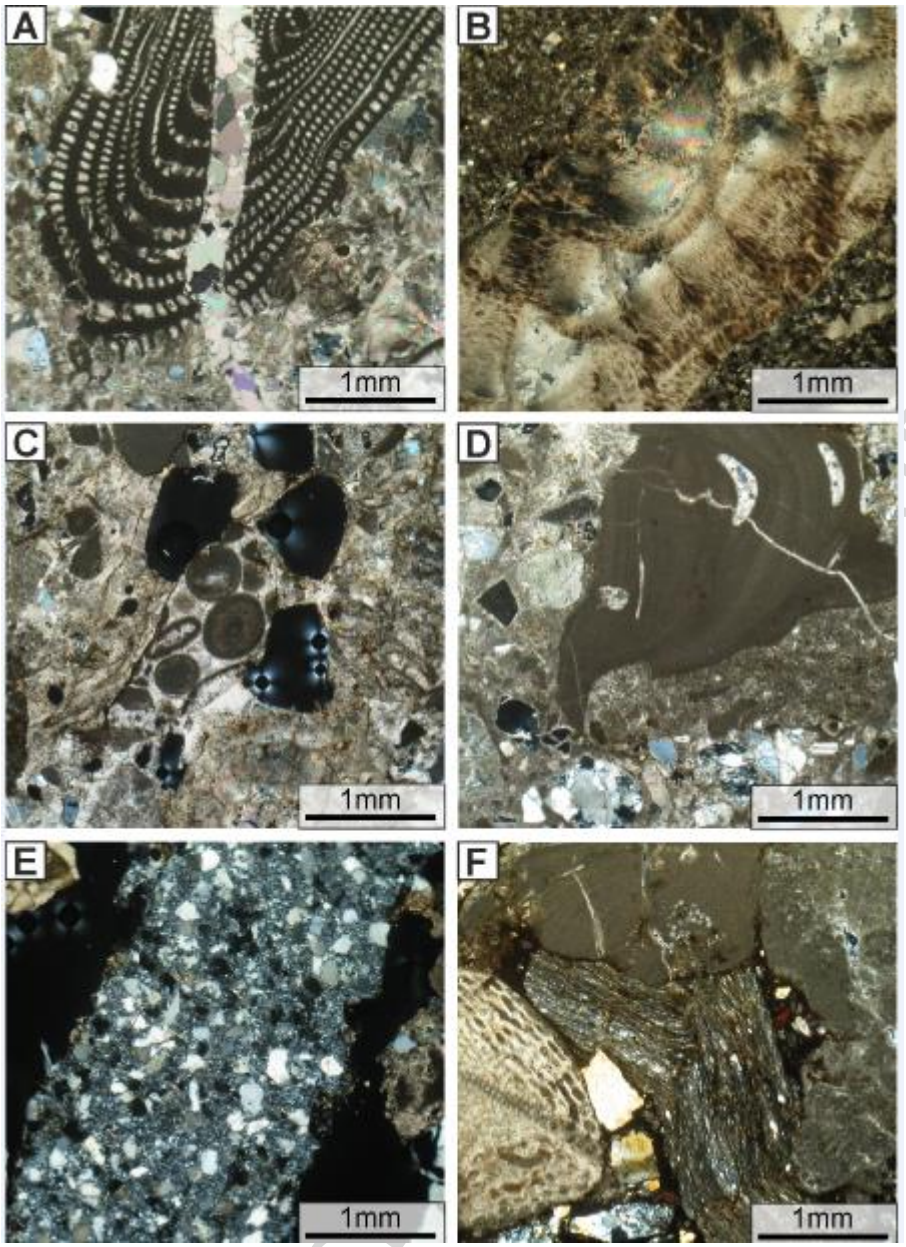

Figure 7

ACCEPTED MANUSCRIPT

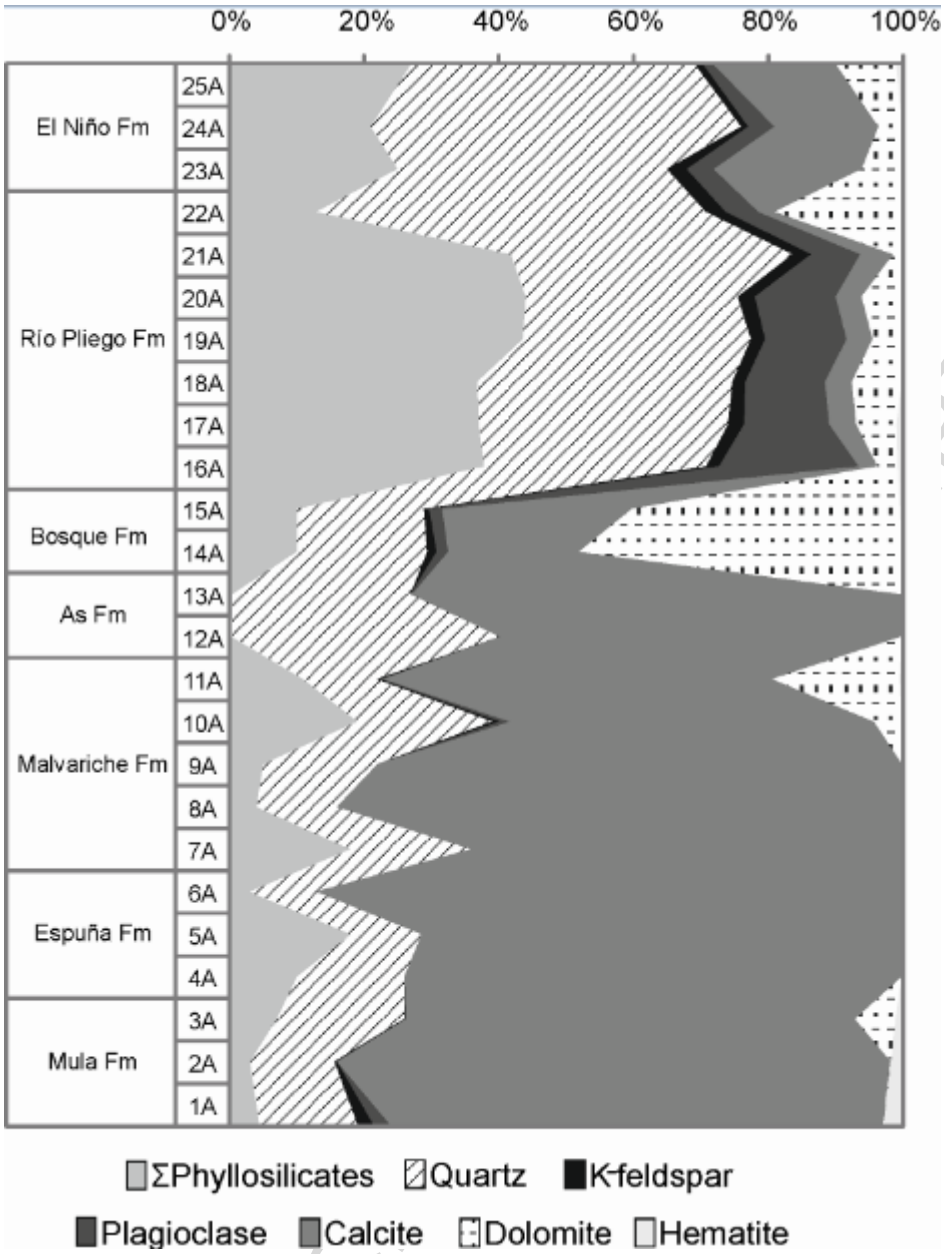

Figure 8

ACCEPTED MANUSCRIPT

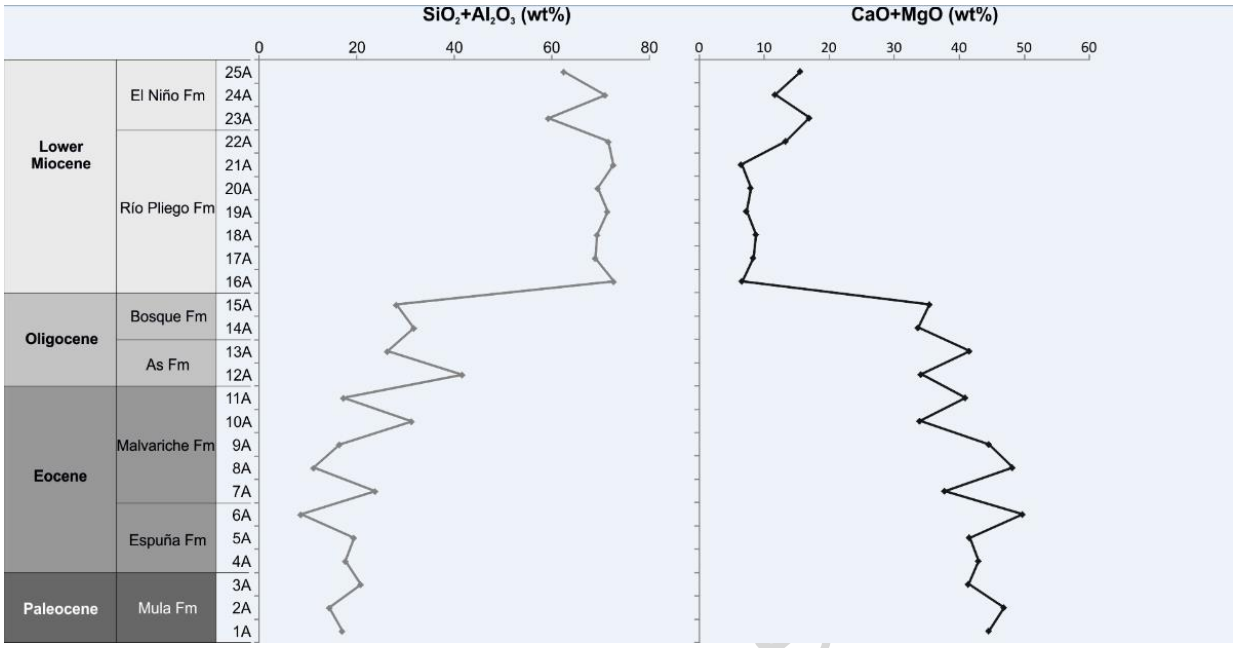

Figure 9

ACCEPTED MANUSCRIPT

ACCEPTED MANUSCRIPT

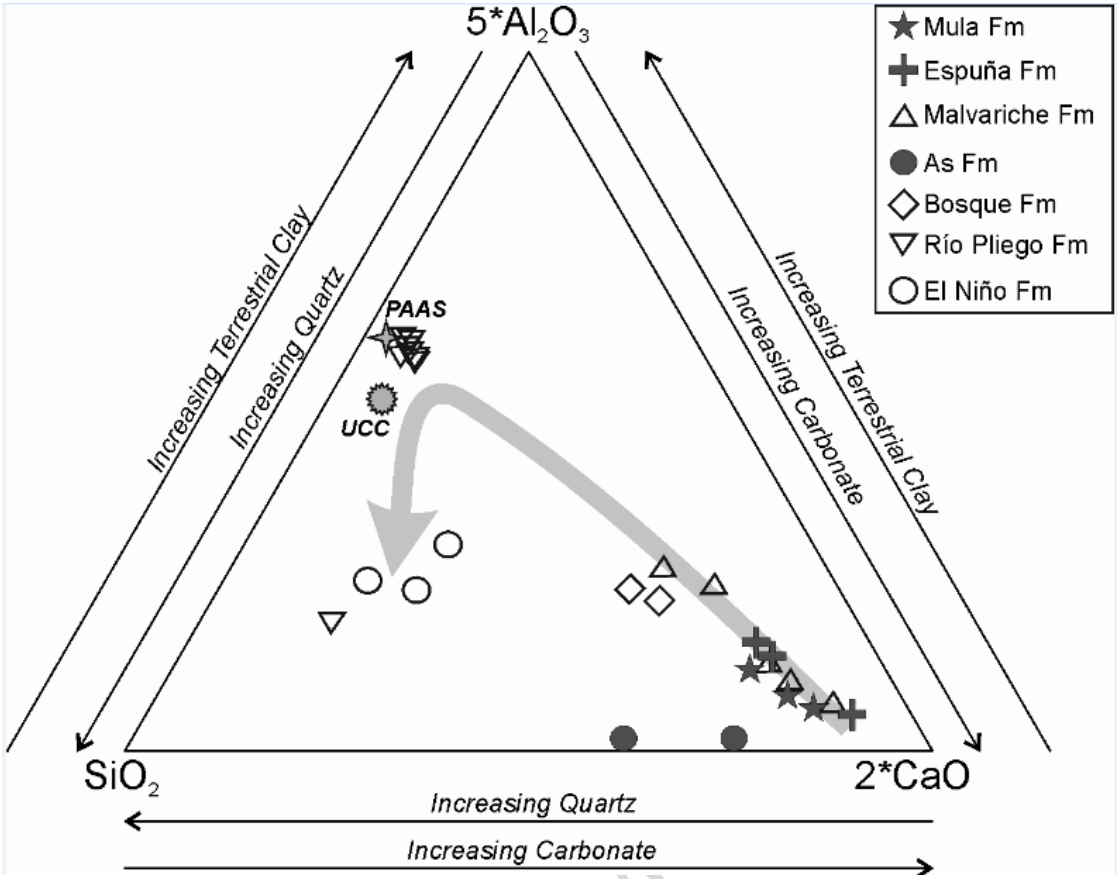

Figure 10

ACCEPTED MANUSCRIPT

ACCEPTED MANUSCRIPT

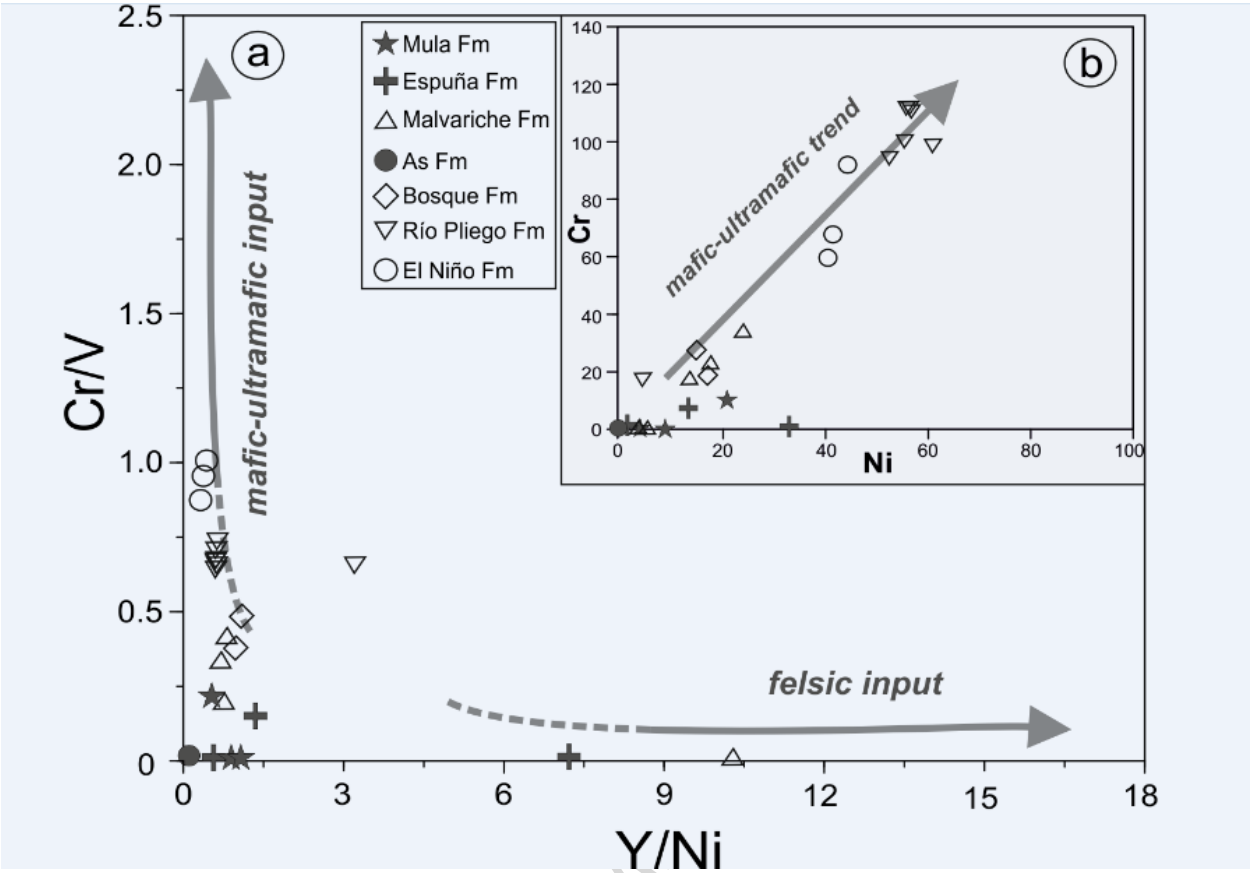

Figure 11

ACCEPTED MANUSCRIPT

ACCEPTED MANUSCRIPT

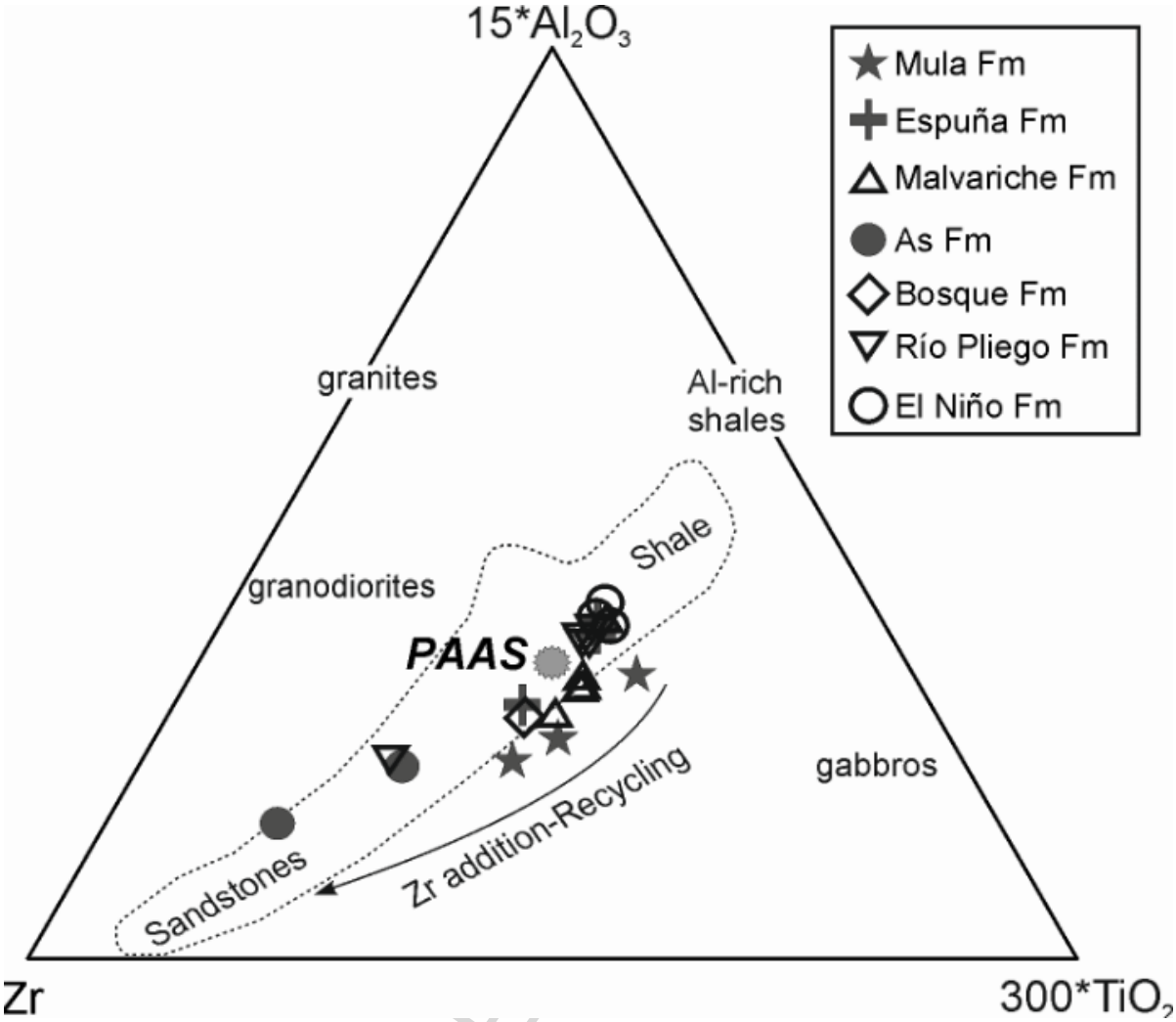

Figure 12

ACCEPTED

ACCEPTED MANUSCRIPT

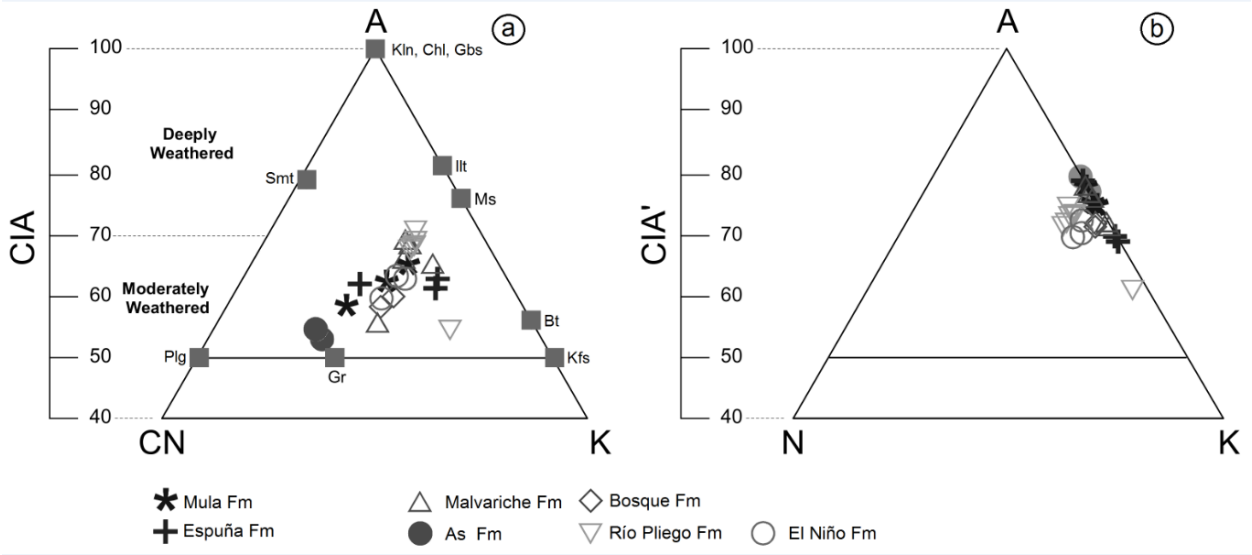

Figure 13

ACCEPTED MANUSCRIPT

ACCEPTED MANUSCRIPT

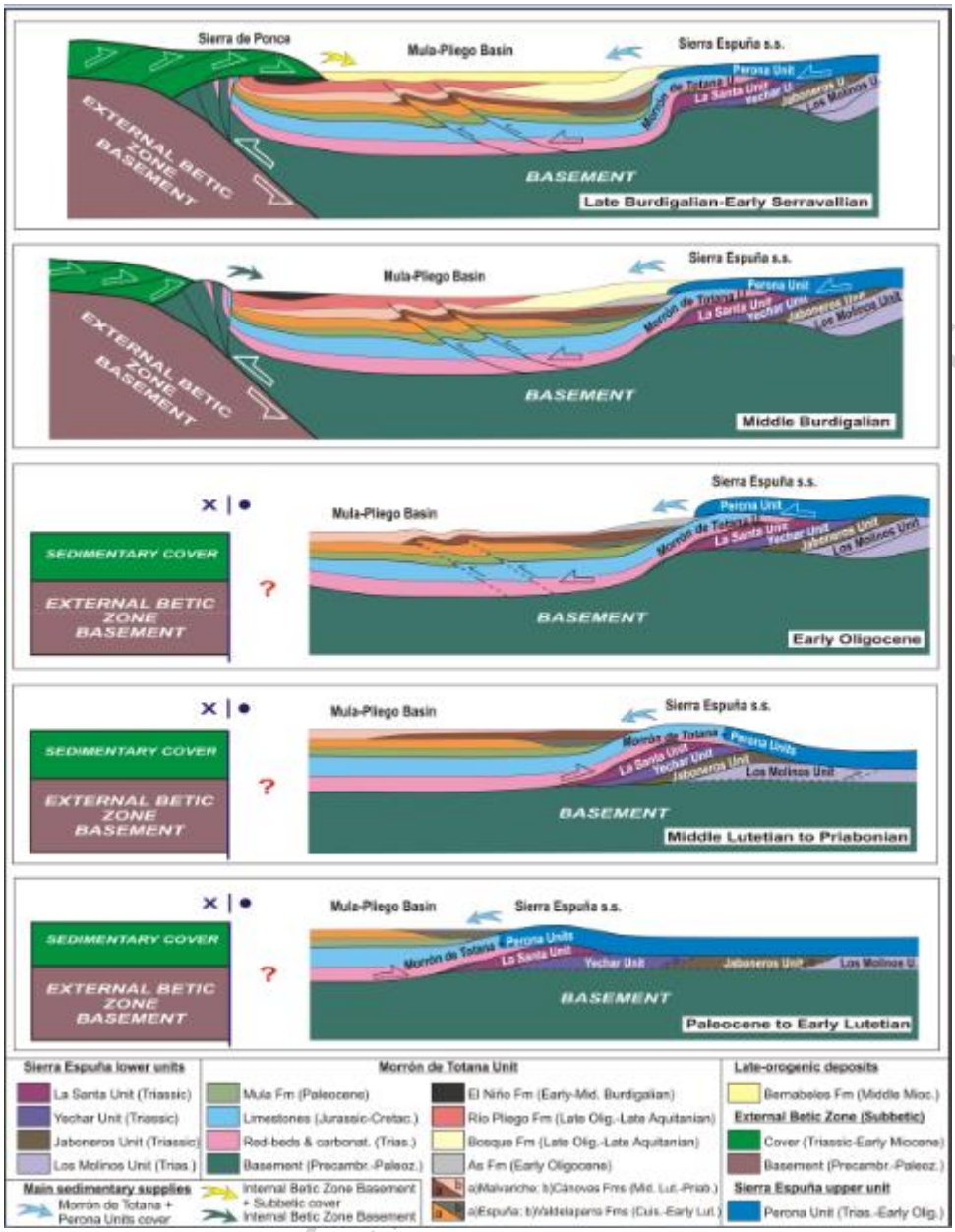

Figure 14

ACCEPTED MANUSCRIPT

Table 1

	Formation	Espuña		As		Río Pliego						El Niño de Mula	
	Sample	**4P**	**5P**	**12P**	**13P**	**16P**	**18P**	**19P**	**20P**	**21P**	**22P**	**23P**	**24P**
		Pre-orogenic cycle				Syn-orogenic cycle							
NCE	**Q**												
	Quartz (single crystal)	132	76	186	132	138	52	64	60	42	204	108	96
	Polycrystalline quartz with tectonic fabric	3	0	5	0	19	2	62	11	9	6	8	10
	Polycrystalline quartz without tectonic fabric	2	0	0	0	5	0	1	0	0	0	1	0
	Quartz in metamorfic r.f.	2	0	4	7	1	13	12	5	1	0	0	2
	Quartz in plutonic r.f.	2	0	0	0	0	0	0	0	0	0	0	0
	Quartz in plutonic or gneissic r.f	0	0	0	0	0	0	0	1	0	0	0	0
	Quartz in sandstone	1	0	0	0	0	1	1	8	1	0	0	0
	Calcite replacement on quartz	0	4	0	0	0	0	5	1	2	9	2	7
	F												
	Feldspar (single crystal)	0	2	0	0	0	0	0	1	0	2	0	0
	M												
	Micas and chlorite (single crystal)	0	0	0	0	3	0	0	0	0	0	0	0
	Micas and chlorite in volcanic r.f.	0	0	0	0	0	0	0	0	0	0	0	0
	Micas and chlorite in metamorfic r.f.	0	0	0	0	1	0	0	1	0	0	0	0
	L												
	Shale	0	0	0	0	0	0	0	0	1	0	0	0
	Slate	0	0	0	0	27	15	47	20	0	0	1	0
	Phyllite	0	0	0	0	37	56	18	43	18	1	1	0
	Fine grained schist	0	0	0	0	0	0	1	2	0	0	0	0
	Metarenite	0	0	0	0	1	0	14	80	4	1	2	3
	Siltstone	0	0	0	0	0	1	4	3	5	0	0	0
	Arenite	0	0	0	0	0	23	2	45	26	0	0	1
	Chert	0	1	1	0	1	0	0	1	3	12	5	8
	Metasiltite	0	0	0	0	0	0	0	3	0	0	0	0
NCI	Fe-oxide	0	0	1	1	0	17	7	3	0	0	0	0
CI	Bioclast	158	220	4	6	11	6	2	0	15	0	0	0
CE	Micritic limestone	0	0	8	9	5	33	6	2	16	7	14	21
	Sparitic limestone	0	0	8	0	0	1	0	1	11	3	1	0
	Microsparitic limestone	0	0	0	0	3	1	0	0	7	11	7	9
	Biosparitic limestone	0	0	0	0	1	3	0	0	10	0	0	0
	Biomicritic limestone	0	0	0	0	8	55	20	0	25	0	0	0
	Ooid grainstone	0	0	0	0	0	2	0	0	8	0	0	1
	Packstone	0	0	0	0	0	3	8	0	2	0	0	0
	Fossil (single skeleton)	0	0	138	156	18	35	19	4	65	2	31	25
	Fossil in limestone or dolostone	0	0	0	0	0	11	0	2	8	0	0	0
	Single spar (calcite)	0	0	0	0	0	0	4	0	1	30	17	21
Mx	Siliciclastic matrix	0	0	0	0	84	15	25	61	36	0	1	3
	Carbonate matrix	0	0	81	126	0	4	0	0	0	0	0	0
	Epi-matrix	0	0	0	0	1	0	0	0	0	0	0	1
	Pseudo-matrix	0	0	0	0	25	0	0	0	1	0	0	0
	Secondary matrix	0	0	0	0	0	0	0	0	5	0	0	0
Cm	Carbonate cement (pore-filling)	212	222	146	113	0	0	1	0	5	38	127	105
	Carbonate cement (patchy calcite)	2	0	1	0	0	0	0	0	0	0	0	0
	Carbonate cement (fracture/vein)	72	0	3	10	0	0	1	0	0	0	0	0
	Hematitic cement (Fe-oxide cement)	0	0	0	0	0	0	0	327	3	0	0	0
	Siliceous cement	0	0	0	0	0	1	0	0	0	0	0	0

ACCEPTED MANUSCRIPT

ACCEPTED MANUSCRIPT

Other grains	Calcite replacement on undetermined grain	0	0	1	0	10	7	2	7	6	11	98	111
	Undetermined grain	0	1	0	0	12	0	1	14	24	3	7	1
TOT		586	526	587	560	411	357	327	706	360	340	431	425

ACCEPTED MANUSCRIPT

ACCEPTED MANUSCRIPT

Table 2

Formation	Sample	%			%			%			%			%			%			%		
		NCE	CI	CE	Qm	F	Lt+CE	Lm	Lss	Lsc(CE)	Lm	Ls+CE	CI	Rm	CE	Rss	Rg	Rs+CE	Rm	Qt	F	L
El Niño	24P	62.4	0.0	37.6	58.3	0.0	41.7	13.1	9.1	77.8	13.1	86.9	0.0	14.9	76.2	8.9	0.0	85.1	14.9	60.0	0.0	40.0
	23P	65.9	0.0	34.1	63.2	0.0	36.8	13.8	5.7	80.5	13.8	86.2	0.0	13.8	80.5	5.7	0.0	86.2	13.8	60.5	0.0	39.5
Río Pliego	22P	81.1	0.0	18.9	73.7	0.7	25.6	10.7	16.0	73.3	10.7	89.3	0.0	10.7	73.3	16.0	0.0	89.3	10.7	79.4	0.7	19.9
	21P	42.1	4.9	53.0	20.5	0.0	79.5	13.7	15.4	70.9	12.8	81.0	6.2	14.0	70.3	15.7	0.0	86.0	14.0	20.1	0.0	79.9
	20P	97.1	0.0	2.9	24.8	0.3	74.9	73.3	22.6	4.1	73.3	26.7	0.0	71.4	3.9	24.7	0.4	28.4	71.1	28.3	0.3	71.3
	19P	79.4	0.7	19.9	30.4	0.0	69.6	68.9	2.9	28.2	68.3	30.8	1.0	70.3	26.5	3.2	0.0	29.7	70.3	50.2	0.0	49.8
	18P	52.1	1.9	46.0	24.3	0.0	75.7	30.3	10.0	59.8	29.6	68.0	2.4	33.7	56.5	9.8	0.0	66.3	33.7	22.1	0.0	77.9
	16P	83.6	3.9	12.5	56.3	0.0	43.7	70.0	0.8	29.2	64.1	27.5	8.4	70.5	28.7	0.8	0.0	29.5	70.5	61.9	0.0	38.1
As	13P	44.8	1.9	53.2	93.9	0.0	6.1	0.0	0.0	100.0	0.0	96.5	3.5	4.1	95.9	0.0	0.0	95.9	4.1	45.7	0.0	54.3
	12P	58.0	1.2	40.8	89.6	0.0	10.4	3.1	0.6	96.3	3.0	94.5	2.4	5.5	93.9	0.6	0.0	94.5	5.5	56.0	0.0	44.0
España	5P	27.6	72.4	0.0	95.2	2.4	2.4	0.0	0.0	0.0	0.0	0.5	99.5	0.0	0.0	0.0	0.0	0.0	0.0	96.4	2.4	1.2
	4P	47.3	52.7	0.0	96.5	0.0	3.5	100.0	0.0	0.0	1.9	0.0	98.1	83.3	0.0	16.7	25.0	12.5	62.5	100.0	0.0	0.0

ACCEPTED MANUSCRIPT

Table 3

Formation	Sample	Exp (I/S+C/S)	Illite and micas	Kaol	Chl	ΣPhyll	Qtz	K-feld	Plg	Calc	Dol	Hem
El Niño	**25A**	1	22	0	2	25	46	1	2	18	7	0
	24A	0	17	0	4	21	55	1	4	16	4	0
	23A	0	20	0	5	25	41	3	4	21	6	0
Río Pliego	**22A**	0	10	1	2	13	57	3	5	3	19	0
	21A	0	30	5	7	42	42	3	7	5	1	0
	20A	0	33	5	6	44	31	3	12	4	6	0
	19A	0	33	5	6	44	34	2	12	4	4	0
	18A	0	23	6	8	37	38	2	12	4	7	0
	17A	0	26	5	6	37	37	2	13	4	6	1
	16A	0	27	5	6	38	33	2	21	3	3	1
El Bosque	**15A**	0	6	2	2	10	19	1	2	28	40	0
	14A	0	6	2	2	10	19	1	2	20	48	0
As	**13A**	0	tr	0	0	tr	26	0	0	73	0	0
	12A	0	tr	0	0	tr	40	0	0	60	0	0
Malvariche	**11A**	0	8	2	1	11	11	1	1	58	19	0
	10A	tr	15	3	tr	19	20	1	2	54	4	0
	9A	0	5	0	0	5	17	0	0	78	0	0
	8A	0	4	0	0	4	12	0	0	84	0	0
	7A	0	18	0	0	18	18	0	0	64	0	0
Espuña	**6A**	0	3	0	0	3	10	0	0	87	0	0
	5A	0	18	0	0	18	11	0	0	71	0	0
	4A	0	10	0	0	10	16	0	0	74	0	0
Mula	**3A**	0	7	0	0	7	19	0	0	67	6	1
	2A	0	3	0	0	3	13	0	0	82	0	2
	1A	0	4	0	0	4	14	2	2	77	0	3

Legend: Exp - expandable clay minerals (I/S, illite-smectite; C/S, chlorite-smectite); Kaol - kaolinite; Chl - chlorite; Phyll - phyllosilicates; Qtz - quartz; K-feld - K-feldspar; Plg - plagioclase; Calc - calcite; Dol - dolomite; Hem - hematite; tr - trace.

ACCEPTED MANUSCRIPT

ACCEPTED MANUSCRIPT

Table 4

Formation	*Mula*			*Espuña*			*Malvariche*					*As*		*El Bosque*		*Rio Pliego*							*El Niño*		
Sample	**1A**	**2A**	**3A**	**4A**	**5A**	**6A**	**7A**	**8A**	**9A**	**10A**	**11A**	**12A**	**13A**	**14A**	**15A**	**16A**	**17A**	**18A**	**19A**	**20A**	**21A**	**22A**	**23A**	**24A**	**25A**
Oxides (wt%)																									
Na_2O	0.00	0.00	0.01	0.00	0.00	0.00	0.00	0.00	0.00	0.01	0.00	0.00	0.00	0.10	0.07	0.84	0.63	0.68	1.12	0.99	0.67	0.08	0.31	0.19	0.31
MgO	1.11	0.88	1.54	1.16	1.24	0.73	1.33	0.92	0.83	1.69	1.94	0.51	0.70	7.13	6.68	3.07	3.24	3.32	2.99	3.39	2.43	5.04	2.55	1.76	2.48
Al_2O_3	1.94	1.45	2.75	3.26	3.70	1.21	5.90	1.66	2.49	6.59	2.91	0.20	0.26	4.91	4.52	18.02	16.75	16.50	17.27	17.39	16.90	3.61	6.92	5.64	5.13
SiO2	15.10	2.98	18.11	4.46	5.73	7.37	17.92	9.55	3.99	24.69	4.442	1.48	6.07	26.86	3.64	54.70	52.20	52.85	54.16	52.09	55.78	68.05	52.43	65.34	57.38
P_2O_5	0.04	0.04	0.04	0.18	0.18	0.02	0.01	0.02	0.03	0.06	0.66	0.01	0.02	0.04	0.04	0.11	0.12	0.11	0.10	0.10	0.06	0.03	0.09	0.06	0.07
K_2O	0.354	0.317	0.573	0.911	1.074	0.214	1.463	0.300	0.505	1.275	0.753	0.033	0.054	1.182	1.077	3.54	3.36	3.29	3.45	3.48	3.12	1.41	1.60	1.22	1.16
CaO	43.45	6.02	9.887	1.82	0.34	9.03	6.47	7.30	3.76	2.266	9.03	3.63	0.88	6.57	8.77	3.53	5.09	5.45	4.30	4.56	4.05	8.29	14.42	9.94	13.09
TiO_2	0.16	0.12	0.19	0.17	0.18	0.07	0.29	0.10	0.17	0.04	0.18	0.01	0.02	0.32	0.29	0.89	0.87	0.84	0.89	0.91	0.86	0.20	0.35	0.26	0.25
MnO	0.01	0.00	0.01	0.00	0.00	0.00	0.01	0.01	0.01	0.00	0.01	0.00	0.00	0.03	0.02	0.05	0.06	0.05	0.06	0.06	0.05	0.03	0.07	0.05	0.08
Fe_2O_3	1.183	0.893	1.386	1.366	1.662	0.722	3.232	1.086	1.467	3.075	3.355	0.019	0.333	1.993	1.833	6.49	7.74	6.73	6.42	6.66	7.05	1.38	3.25	2.40	2.64
L.O.I.	6.029	7.277	4.769	6.647	5.619	9.866	2.999	9.035	5.591	9.239	5.609	3.539	1.388	0.455	2.233	8.00	9.55	9.62	8.53	9.49	8.32	11.22	17.78	12.62	16.71
TOT%	99.38	99.97	99.23	99.80	99.72	99.22	99.60	99.97	99.15	99.29	98.255	99.65	99.72	99.58	99.17	99.25	99.63	99.45	99.30	99.12	99.29	99.34	99.77	99.47	99.30
Trace elements (ppm)																									
Ni	95.1	56.8	21.17	13.79	33.08	16.6	18.06	4.15	0.97	24.26	13.95	nd	nd	15.244	17.34	57.05	61.01	61.04	55.61	56.45	52.64	2.54	44.41	41.72	40.688
Cr	nd	nd	11	8	nd	nd	23	nd	nd	34	189	nd	nd	28	19	111	99	99	101	112	95	16	92	68	60
V	31	25	151	53	49	80	68	41	34	83	99	9	12	59	53	161	152	151	154	157	141	24	94	72	70
La	nd	nd	nd	nd	nd	nd	nd	nd	nd	nd	nd	nd	nd	nd	nd	46	45	44	50	50	41	nd	25	nd	16
Ce	nd	28	35	39	36	34	58	39	38	62	27	nd	16	52	49	113	104	110	103	106	99	32	49	39	38
Co	nd	nd	3.42	3.42	3.42	nd	3.42	nd	3.42	3.42	3.42	nd	nd	3.42	3.42	18.34	20.70	18.10	21.14	18.58	18.08	4.93	6.87	8.98	10.10
Ba	nd	528	123	12	26	nd	nd	nd	nd	146	30	nd	nd	146	100	570	597	549	584	595	582	219	266	241	569
Nb	n	4	7	5	5	4	9	4	4	9	4	1	2	8	8	19	18	18	19	18	18	6	9	7	6

ACCEPTED MANUSCRIPT

	d																								
Y	nd	5	11	19	18	12	12	11	10	22	11	5	4	17	17	35	35	35	35	36	34	9	19	13	14
Sr	nd	212	194	292	324	295	235	116	123	480	114	258	451	294	307	170	285	307	186	223	133	60	514	369	535
Zr	nd	43	35	39	40	26	63	27	50	100	46	14	10	111	101	212	206	210	220	222	218	139	75	56	56
Cu	nd	19.43	18.50	8.83	14.26	3.87	6.09	14.01	9.70	4.34	16.46	nd	5.97	7.66	nd	25.50	17.86	23.18	17.68	22.54	14.99	2.08	29.55	22.75	23.28
Zn	nd	24.47	43.68	74.27	54.93	21.63	55.76	31.06	42.10	51.59	48.14	14.73	21.51	42.79	44.46	######	######	######	######	######	######	30.79	######	79.29	88.82
Rb	nd	713	429	742	347	316	692	136	222	967	430	3	4	950	447	167	155	150	160	160	139	339	80	557	555
Ratios																									
CIA	59	65	62	63	61	62	65	69	66	68	56	55	53	60	58	69	68	68	67	68	71	54	63	63	60
CIA'	78	75	75	70	69	79	72	78	76	77	71	79	77	71	72	73	73	73	71	72	74	61	70	72	70

Legend: CIA - Chemical Index of Alteration (Nesbitt and Young, 1982); CIA' - Chemical Index of Alteration', without calcium (Perri et al., 2014); nd - not detected.

ACCEPTED MANUSCRIPT

ACCEPTED MANUSCRIPT

Highlights

- We examine Cenozoic sediments of the Malaguide Complex, Betic Cordillera
- Stratigraphic relations and petrological and geochemical signatures are used
- We study the sedimentary evolution to evaluate erosional exhumation from pre-to-syn-orogenic stages
- The exhumation history reveals the Paleocene to Miocene geodynamic evolution of the Malaguide Complex

ACCEPTED MANUSCRIPT

The author has requested enhancement of the downloaded file. All in-text references underlined in blue are linked to publications on ResearchGate.